

1  
2  
3  
4  
5  
6  
7  
8  
9  
10  
11  
12  
13  
14  
15  
16  
17  
18  
19  
20  
21  
22  
23  
24  
25  
26  
27  
28  
29  
30  
31  
32  
33  
34  
35  
36  
37  
38  
39  
40  
41  
42  
43  
44  
45  
46  
47  
48  
49  
50  
51  
52  
53  
54  
55

# Hydroxybiphenylamide GroEL/ES inhibitors are potent antibacterials against planktonic and biofilm forms of *Staphylococcus aureus*.

## AUTHOR NAMES

Trent Kunkle,<sup>a,1</sup> Sanofar Abdeen,<sup>a,1</sup> Nilshad Salim,<sup>a</sup> Anne-Marie Ray,<sup>a</sup> McKayla Stevens,<sup>a</sup>  
Andrew J. Ambrose,<sup>b</sup> José Victorino,<sup>a</sup> Yangshin Park,<sup>a,c,d</sup> Quyen Q. Hoang,<sup>a,c,d</sup> Eli Chapman,<sup>b</sup>  
and Steven M. Johnson<sup>a,\*</sup>

<sup>1</sup> Co-first author

## AUTHOR ADDRESSES

<sup>a</sup> Indiana University School of Medicine, Department of Biochemistry and Molecular Biology,  
635 Barnhill Dr., Indianapolis, IN 46202

<sup>b</sup> The University of Arizona, College of Pharmacy, Department of Pharmacology and  
Toxicology, 1703 E. Mabel St., PO Box 210207, Tucson, AZ 85721

<sup>c</sup> Stark Neurosciences Research Institute, Indiana University School of Medicine. 320 W. 15th  
Street, Suite 414, Indianapolis, IN 46202

<sup>d</sup> Department of Neurology, Indiana University School of Medicine. 635 Barnhill Drive,  
Indianapolis, IN 46202

## KEYWORDS.

GroEL, GroES, HSP60, HSP10, molecular chaperone, chaperonin, proteostasis, small molecule  
inhibitors, *ESKAPE* pathogens, MRSA, antibiotics.

---

This is the author's manuscript of the article published in final edited form as:

Kunkle, T., Abdeen, S., Salim, N., Ray, A.-M., Stevens, M., Ambrose, A. J., ... Johnson, S. M. (2018).  
Hydroxybiphenylamide GroEL/ES inhibitors are potent antibacterials against planktonic and biofilm forms of  
*Staphylococcus aureus*. *Journal of Medicinal Chemistry*. <https://doi.org/10.1021/acs.jmedchem.8b01293>

**ABSTRACT**

We recently reported the identification of a GroEL/ES inhibitor (**1**: *N*-(4-(benzo[*d*]thiazol-2-ylthio)-3-chlorophenyl)-3,5-dibromo-2-hydroxybenzamide) that exhibited *in vitro* antibacterial effects against *Staphylococcus aureus* comparable to vancomycin, an antibiotic of last resort. To follow-up, we have synthesized 43 compound **1** analogs to determine the most effective functional groups of the scaffold for inhibiting GroEL/ES and killing bacteria. Our results identified that the benzothiazole and hydroxyl groups are important for inhibiting GroEL/ES-mediated folding functions, with the hydroxyl essential for antibacterial effects. Several analogs exhibited >50-fold selectivity indices between antibacterial efficacy and cytotoxicity to human liver and kidney cells in cell culture. We found that MRSA were not able to easily generate acute resistance to lead inhibitors in a gain-of-resistance assay, and that lead inhibitors were able to permeate through established *S. aureus* biofilms and maintain their bactericidal effects.

## INTRODUCTION:

In 2013, the Centers for Disease Control and Prevention (CDC) released a report highlighting the dangers posed by multi-drug resistant bacteria, in particular a group of six that have been termed the **ESKAPE** pathogens: *Enterococcus faecium* (Gram-positive), *Staphylococcus aureus* (Gram-positive), *Klebsiella pneumoniae* (Gram-negative), *Acinetobacter baumannii* (Gram-negative), *Pseudomonas aeruginosa* (Gram-negative), and the *Enterobacter* species (Gram-negative).<sup>1</sup> The report estimated that these bacteria infect over two-million people in the U.S. annually, leading to ~23,000 deaths. Of the **ESKAPE** pathogens, methicillin-resistant strains of *S. aureus* (MRSA) were found to be the deadliest, causing ~80,000 infections and ~11,000 deaths annually. Unfortunately, the development of new antibiotics over the past four decades has continually declined, and continuing research programs tend to focus on re-derivatizing already known antibacterial classes.<sup>2-4</sup> In addition, many bacteria are intrinsically able to evade antibiotic effects by forming biofilms, which are often hallmarks of chronic infections.<sup>5</sup> While vancomycin is effective at treating planktonic *S. aureus*, it is not able to penetrate and kill bacteria within biofilms.<sup>6,7</sup> Thus, to circumvent these resistance mechanisms, there is an urgent need for antibacterials that function through new mechanisms of action and previously unexploited pathways.

While disrupting protein homeostasis has proven to be an effective antibacterial strategy in the context of inhibiting the transcriptional and translational machineries, perturbing protein folding pathways has gone largely unexplored.<sup>3</sup> To facilitate newly synthesized polypeptides folding into their active/native structural conformations, cells utilize a class of accessory proteins termed molecular chaperones, also known as Heat Shock Proteins (HSPs).<sup>8</sup> When molecular chaperone functions are compromised, non-native polypeptides could misfold and aggregate,

1  
2  
3 which is detrimental to cell viability.<sup>9-12</sup> Thus, targeting molecular chaperones with small  
4 molecule inhibitors should be an effective strategy for killing bacteria that is unique from the  
5 mechanisms of current antibiotics. While significant efforts have been made to target HSP70  
6 and HSP90 chaperones for developing anti-cancer agents, researchers are now beginning to  
7 explore these chaperones as antibiotic targets.<sup>13-20</sup> However, targeting HSP60 chaperonin  
8 systems, called GroEL chaperonins in bacteria, has gone largely unexplored. GroEL is a homo-  
9 tetradecameric protein complex that consists of two, seven-membered rings that stack back-to-  
10 back with each other. GroEL functions to refold nascent polypeptides through a mechanism  
11 unique from other molecular chaperones. To facilitate the folding of substrate polypeptides,  
12 GroEL requires binding of ATP and a co-chaperone, called GroES. GroES binding to the GroEL  
13 apical domains encapsulates the substrate polypeptides within the central cavity of GroEL, where  
14 they can attempt to fold while being sequestered from the outside environment. Details of the  
15 GroEL/ES-mediated folding cycle have been extensively investigated and reported elsewhere.<sup>21-</sup>

16  
17  
18  
19  
20  
21  
22  
23  
24  
25  
26  
27  
28  
29  
30  
31  
32  
33  
34  
35  
36  
37  
38  
39  
40  
41  
42  
43  
44  
45  
46  
47  
48  
49  
50  
51  
52  
53  
54  
55  
56  
57  
58  
59  
60

Since the GroEL/ES system is essential for bacterial viability under all conditions, we  
hypothesize that blocking its functions with small molecule inhibitors should be an effective  
antibacterial strategy.<sup>28,29</sup> A caveat to this strategy is that human HSP60 is moderately  
conserved with the bacterial homologs (48% identity with the prototypical GroEL chaperonin  
from *Escherichia coli*), which raises the question of potential off-target effects against human  
cells. However, HSP60 is localized within the mitochondrial matrix of human cells, which is  
highly impermeable to small molecules. Thus, even if compounds can inhibit HSP60 *in vitro*,  
they may not reach and inhibit it in the mitochondrial matrix, permitting selective targeting of  
bacteria over human cells.

1  
2  
3 In a previous study, we performed high-throughput screening and identified 235  
4 inhibitors of the GroEL/ES folding cycle.<sup>30</sup> In a follow-up study evaluating a subset of these  
5 GroEL/ES inhibitors for their antibacterial effects against the *ESKAPE* pathogens, we identified  
6 compound **1** (**Figure 1A**) as a hit candidate for further antibacterial development.<sup>31</sup> In particular,  
7 compound **1** exhibited bactericidal effects against *S. aureus* that were comparable to vancomycin  
8 (i.e. sub- $\mu$ M EC<sub>50</sub>). While compound **1** exhibited low-to-moderate cytotoxicity against human  
9 liver (THLE-3) and kidney (HEK 293) cell lines, it still had >50-fold selectivity indices for  
10 killing *S. aureus* bacteria. Intriguingly, compound **1** has been reported to have anthelmintic  
11 activity against *Trichocephalus muris*, and two anthelmintic drugs used to treat parasitic  
12 infections in livestock, closantel and rafoxanide (**Figure 1B**), bear striking resemblances to the  
13 compound **1** scaffold.<sup>32, 33</sup> In addition, Cheng *et al.* reported similar analogs that exhibited anti-  
14 MRSA activities, although the reported structure-activity relationships (SAR) suggested that  
15 their antibacterial effects were not entirely through targeting transglycosylase activity.<sup>34</sup> Thus,  
16 there is a high probability that targeting the GroEL/ES chaperonin system could be contributing  
17 significantly to its antibacterial effects, which warrants further investigation.

18  
19 While compound **1** itself is a promising GroEL/ES inhibitor to take forward as an anti-  
20 bacterial candidate, there is room for further optimization before proceeding into a proof-of-  
21 principle anti-bacterial efficacy models in animals (e.g. mice systemically infected with *S.*  
22 *aureus*). As a first step in our optimization strategy, rather than adding various substituents and  
23 substructures to the scaffold as is often done in drug development, we chose an opposite  
24 approach and employed a molecular deconstruction strategy where we systematically removed  
25 the various substituents and substructures (**R<sup>1</sup>-R<sup>5</sup> – Figure 1A**) to evaluate their contributions to  
26 inhibitor potency and selectivity. Thus, we synthesized a library of 43 analogs that contained all  
27  
28  
29  
30  
31  
32  
33  
34  
35  
36  
37  
38  
39  
40  
41  
42  
43  
44  
45  
46  
47  
48  
49  
50  
51  
52  
53  
54  
55  
56  
57  
58  
59  
60

1  
2  
3 the different  $\pm$  combinations of the **R<sup>1</sup>-R<sup>5</sup>** groups. We then tested them in a series of assays to  
4  
5 achieve three primary objectives: 1) determine which groups are crucial to inhibit GroEL/ES and  
6  
7 HSP60/10 folding function *in vitro*; 2) identify groups that expand the therapeutic window  
8  
9 further between antibacterial efficacy and human cell cytotoxicity; and 3) determine if inhibitors  
10  
11 are effective against bacteria in biofilms, and whether or not bacteria will be able to generate  
12  
13 acute resistance to this molecular class. Results from these assays would then allow us to  
14  
15 identify the smallest effective inhibitor analog that maintains potency against bacteria while  
16  
17 reducing cytotoxicity to human cells. Knowing this information would then allow us to build  
18  
19 upon this base scaffold in a more rational approach to improve the pharmacological properties of  
20  
21 this antibacterial series.  
22  
23  
24  
25  
26  
27

## 28 **RESULTS AND DISCUSSION**

### 29 **Evaluating the effectiveness of compound 1 analogs for inhibiting the GroEL/ES-mediated** 30 31 **folding cycle.** 32 33 34

35 As a first step in this study, we synthesized analogs **1-44** using well-established chemistry  
36  
37 as outlined in **Scheme 1**. A nucleophilic aromatic substitution reaction between 2-  
38  
39 mercaptobenzothiazole and 3,4-dichloronitrobenzene was employed to give the nitro-  
40  
41 intermediate **45** (containing the chloro-group in the **R<sup>2</sup>** position), which was subsequently  
42  
43 reduced to the amine **46** using tin powder in a 10% mixture of HCl in AcOH.<sup>32, 35-38</sup> The  
44  
45 intermediate amine **47**, lacking the chloro-group at the **R<sup>2</sup>** position, was synthesized in one step  
46  
47 by a nucleophilic aromatic substitution reaction between 2-chlorobenzothiazole and  
48  
49 aminothiophenol.<sup>39</sup> Compounds **17-44** were prepared by reacting the respective aryl-acid  
50  
51 chlorides (where commercially available) with amines **46** or **47** with pyridine in anhydrous  
52  
53  
54  
55  
56  
57  
58  
59  
60

1  
2  
3 dicloromethane.<sup>36, 37</sup> If only the respective aryl-carboxylic acids were commercially available,  
4 we either converted them to their acid chloride counter-parts by reacting with thionyl chloride, or  
5  
6 coupled the acids directly to the amines using amide coupling procedures with DDC, DMAP,  
7  
8 and pyridine, or EDC, HOBt•H<sub>2</sub>O, and TEA in dichloromethane.<sup>37</sup> The methoxy-bearing  
9  
10 analogs (**29-44**) were then further de-methylated to analogs **1-16** using BBr<sub>3</sub> in anhydrous  
11  
12 dichloromethane.<sup>36-38, 40</sup> Detailed synthetic protocols and compound characterizations (e.g. <sup>1</sup>H-  
13  
14 NMR, MS, and RP-HPLC) are presented in the Experimental Section and Supporting  
15  
16 Information. We also purchased the two highly related anthelmintic drugs used in veterinary  
17  
18 medicine, closantel and rafoxanide, to determine whether they would also inhibit the GroEL/ES  
19  
20 chaperonin system. While their mode of action is reported to involve uncoupling of the proton  
21  
22 gradient of oxidative phosphorylation, which drives ATP production in the mitochondria of  
23  
24 parasites, it is possible that targeting GroEL/ES or HSP60/10 chaperonin systems could be  
25  
26 contributing to their antibiotic properties.<sup>41, 42</sup>

27  
28  
29  
30  
31  
32  
33 After generating the compound library, we next employed a series of well-established  
34  
35 biochemical assays to evaluate compound inhibitory effects against the GroEL/ES chaperonin  
36  
37 system. As in previous studies, we used *E. coli* GroEL/ES as the surrogate chaperonin system  
38  
39 for refolding of the reporter enzymes malate dehydrogenase (MDH) and rhodanese (Rho).<sup>30, 31, 40</sup>  
40  
41 Briefly, binary complexes are formed between GroEL and denatured MDH or Rho, which are  
42  
43 then refolded to their native states upon addition of ATP and the GroES co-chaperonin.  
44  
45 Enzymatic activities of refolded native MDH or Rho act as coupled reporters of GroEL/ES  
46  
47 refolding functions since in the presence of chaperonin inhibitors, no functional reporter  
48  
49 enzymes are generated. Inhibition IC<sub>50</sub> results for testing of compounds in these two refolding  
50  
51 assays are compiled in **Table 1**, and visually presented in the correlation plot in **Figure 2A**. The  
52  
53  
54  
55  
56  
57  
58  
59  
60

1  
2  
3 log-transformations of  $IC_{50}$  results and standard deviations are presented in **Table S1** in the  
4  
5 Supporting Information. As seen in **Figure 2A**, there is a strong correlation between compounds  
6  
7 inhibiting in the GroEL/ES-dMDH and dRho refolding assays (Spearman correlation coefficient  
8  
9 comparing  $\log(IC_{50})$  values in each assay is 0.9663,  $p < 0.0001$ ), suggesting they are acting on-  
10  
11 target against the chaperonin system. As we do not know where the binding sites are for this  
12  
13 series of inhibitors, precise structure-function interpretation of the results remains elusive. In  
14  
15 general, though, the **R<sup>1</sup>**-benzothiazole coupled with the **R<sup>3</sup>**-hydroxyl are required for potent  
16  
17 inhibition. Halogenation at the **R<sup>2</sup>**-position (Cl) and **R<sup>4</sup>/R<sup>5</sup>** positions (Br) further increases  
18  
19 inhibitor potency, likely through a combination of increased hydrophobic interactions of the  
20  
21 halides themselves, coupled with the electron-withdrawing capability of the bromines lowering  
22  
23 the  $pK_a$  of the salicylate hydroxyl, which could enhance polar interactions within the binding  
24  
25 sites. Perhaps not surprisingly, we found that closantel and rafoxanide were, indeed, potent  
26  
27 GroEL/ES inhibitors; thus, an intriguing question to address in future studies will be how much  
28  
29 does targeting chaperonin systems contribute to the anthelmintic effects of these two veterinary  
30  
31 antibiotics?  
32  
33  
34  
35  
36

37  
38 To further support on-target effects, we evaluated inhibitors against the native MDH and  
39  
40 Rho enzymes to identify false-positives that simply inhibit the reporter reactions of the coupled  
41  
42 refolding assays (detailed procedures are presented in the Supporting Information). While some  
43  
44 compounds were found to inhibit native MDH (e.g. **1**, **5**, closantel, and to lesser extents, **9**, **13**,  
45  
46 and rafoxanide), none of the analogs were found to inhibit native Rho enzymatic activity (**Table**  
47  
48 **1** and **Figure 2B**). While these results further support that inhibitors are targeting the  
49  
50 chaperonin-mediated folding cycle, they also indicate that selectivity issues may be a liability  
51  
52 that future studies would need to address. Hearteningly, though, a few analogs (e.g. compound  
53  
54  
55  
56  
57  
58  
59  
60



1  
2  
3 **2, 3, 6, and 7**) are moderate to potent inhibitors in the GroEL/ES-mediated refolding assays yet  
4  
5 remained inactive against the reporter enzymes, suggesting selectivity concerns are not  
6  
7 insurmountable.  
8  
9

### 12 **Determining the antibacterial effects of compounds against the *ESKAPE* pathogens.**

14  
15 We next evaluated compounds for antibacterial efficacy against the *ESKAPE* pathogens  
16  
17 in liquid media culture as per previously reported procedures.<sup>38</sup> Inhibition EC<sub>50</sub> results for  
18  
19 testing of compounds in these bacterial proliferation assays are shown in **Table 2**. In general,  
20  
21 this series of analogs was ineffective against the Gram-negative bacteria (*K. pneumonia*, *A.*  
22  
23 *baumannii*, *P. aeruginosa*, and *E. cloacae*), likely owing to drug efflux and/or impermeability to  
24  
25 the lipopolysaccharide (LPS) outer membranes of Gram-negative bacteria.<sup>31</sup> However, with  
26  
27 regards to *A. baumannii*, notable exceptions are compounds **2** and **6**, which exhibit EC<sub>50</sub> values  
28  
29 of 2.9 and 12  $\mu$ M, respectively. This suggests that drug efflux and LPS impermeability issues  
30  
31 may not be insurmountable with further inhibitor optimization. As previously observed with  
32  
33 compound **1**, several analogs retained antibacterial efficacy against the Gram-positive bacteria,  
34  
35 *E. faecium* and *S. aureus*, although they were strikingly more effective against *S. aureus*. The  
36  
37 presence of the hydroxyl at the **R**<sup>3</sup> position appears to be integral for potent inhibition of *S.*  
38  
39 *aureus* bacteria, almost regardless of substituents and substructures at the other positions.  
40  
41 However, it is noted that incorporation of the benzothiazole substructure at the **R**<sup>1</sup> position leads  
42  
43 to the most potent inhibitors (and generally required to inhibit *E. faecium*), which may support  
44  
45 on-target effects since these analogs are able to inhibit GroEL/ES-mediated folding functions.  
46  
47  
48  
49  
50  
51 Importantly, these analogs are all equipotent against the MRSA strain that we evaluated  
52  
53  
54  
55  
56  
57  
58  
59  
60

1  
2  
3 compounds against (ATCC #BAA-44, HPV107 designation, isolated from a hospital in Lisbon,  
4  
5 Portugal).

6  
7  
8 When comparing the EC<sub>50</sub> results of this series of compounds against *E. faecium* bacteria  
9  
10 with the IC<sub>50</sub> values obtained in the GroEL/ES-dMDH refolding assay (**Figure 3A**), we note an  
11  
12 almost linear correlation (Spearman correlation coefficient comparing log(I/EC<sub>50</sub>) values in each  
13  
14 assay is 0.9628,  $p < 0.0001$ ), which may indicate on-target effects against GroEL/ES driving  
15  
16 antibacterial activity. When performing the same comparison with MRSA bacteria (**Figure 3B**),  
17  
18 although a trend is evident between antibacterial efficacy and GroEL/ES inhibition MRSA  
19  
20 (Spearman correlation coefficient comparing log(I/EC<sub>50</sub>) values in each assay is 0.8042,  $p <$   
21  
22 0.0001), several compounds that are not GroEL/ES inhibitors still remain effective against  
23  
24 bacteria (e.g. **10-16**). This finding could be a result of *S. aureus* GroEL/ES functioning  
25  
26 differently than the *E. coli* GroEL/ES chaperonin system, which we use as a surrogate in these  
27  
28 studies; however, we cannot rule out potential off-target effects, especially since we know that  
29  
30 some analogs could inhibit MDH and also potentially be targeting transglycosylase as reported  
31  
32 by Cheng *et al.*<sup>34</sup> Further studies are warranted to determine how *E. faecium* and *S. aureus*  
33  
34 GroEL/ES function compared to *E. coli* GroEL/ES, and to identify the specific mechanisms of  
35  
36 action of these inhibitors in both *E. faecium* and *S. aureus* bacteria.  
37  
38  
39  
40  
41  
42  
43

44  
45 **While some GroEL/ES inhibitors can target human HSP60/10 *in vitro*, many display**  
46  
47 **moderate to low cytotoxicity to human cells.**

48  
49 Knowing which compounds were effective GroEL/ES inhibitors with antibacterial  
50  
51 properties, we next evaluated whether they would 1) inhibit human HSP60/10, and 2) exhibit  
52  
53 cytotoxicity to two cell lines that we typically employ for cell viability testing *in vitro*: THLE-3  
54  
55  
56  
57  
58  
59  
60

1  
2  
3 liver cells and HEK 293 kidney cells. These assays were performed as previously reported, with  
4 detailed protocols presented in the Supporting Information.<sup>31, 38, 40</sup> Briefly, the HSP60/10-dMDH  
5 folding assay was conducted analogously to the GroEL/ES-dMDH folding assay so IC<sub>50</sub> results  
6 could be directly compared. The human cell cytotoxicity assays used Alamar Blue reagents to  
7 measure the viability of liver and kidney cells that had been incubated with test compounds over  
8 a 48 h time period. Biochemical inhibition (IC<sub>50</sub>) and cell viability (cytotoxicity; CC<sub>50</sub>) results  
9 for these assays are presented in **Table 3**.

10  
11  
12  
13  
14  
15  
16  
17  
18  
19 While some analogs selectively inhibit *E. coli* GroEL/ES over human HSP60/10 (e.g. **3**,  
20 **4**, **7**, and **8**), IC<sub>50</sub> values between the GroEL/ES-dMDH and HSP60/10-dMDH folding assays  
21 were nearly the same for most analogs (**Figure 4A** - Spearman correlation coefficient comparing  
22 log(IC<sub>50</sub>) values in each assay is 0.8351,  $p < 0.0001$ ). We note, though, that comparison of these  
23 results is convoluted by the fact that some of these analogs also inhibit native MDH, and thus  
24 could be false positives in the HSP60/10-dMDH folding assay owing to simply inhibiting the  
25 MDH reporter reaction. While HSP60/10 inhibition could potentially be teased out by  
26 employing rhodanese as the denatured reporter enzyme as we do in the case of the GroEL/ES-  
27 dRho refolding assay, in our experience, the equivalent HSP60/10-dRho refolding is not as  
28 robust, potentially owing to the lower stability of human HSP60 compared to *E. coli* GroEL.  
29  
30  
31  
32  
33  
34  
35  
36  
37  
38  
39  
40  
41

42  
43  
44  
45  
46  
47  
48  
49  
50  
51  
52  
53  
54  
55  
56  
57  
58  
59  
60  
When comparing the biochemical and cell-based results, there does not appear to be a  
noticeable correlation between HSP60/10-dMDH refolding assay IC<sub>50</sub> values and liver and  
kidney cell viability assay CC<sub>50</sub> values (**Figure 4B** - (Spearman correlation coefficient values are  
0.4791 ( $p < 0.0008$ ) and 0.3286 ( $p < 0.0258$ ) when comparing HSP60/10-dMDH refolding assay  
log(IC<sub>50</sub>) values with liver and kidney cell viability log(CC<sub>50</sub>) values, respectively).  
Interestingly, compounds that bear the **R**<sup>1</sup> benzothiazole and **R**<sup>3</sup> hydroxyl substructures (**1-8**) are

1  
2  
3 generally less cytotoxic against the HEK 293 cells than their counterparts without the **R**<sup>1</sup>  
4 benzothiazole (**9-16**), and also less cytotoxic to the THLE-3 liver cells. Since inclusion of these  
5 two substructures generally afforded more potent chaperonin inhibitors, the differences between  
6 these results may suggest that compound cytotoxicities are predominantly a result of off-target  
7 effects and not from targeting HSP60/10 itself. This would not be surprising since some analogs  
8 are also able to inhibit native MDH (e.g. **1**, **5**, **9**, **13**, closantel, and rafoxanide). When comparing  
9 EC<sub>50</sub> values of compounds inhibiting the proliferation of susceptible and methicillin-resistant *S.*  
10 *aureus* with cell viability CC<sub>50</sub> values against the human liver and kidney cells (**Figure 4C**), we  
11 note that many analogs exhibit >50-fold selectivity indices. Considering we have only been  
12 looking at the effects that removing substituents and substructures have on the potency and  
13 selectivity of this series of analogs, these are exciting initial results to move forward from in  
14 future med-chem efforts where we begin to append and optimize the various substituents and  
15 substructures of this scaffold.  
16  
17  
18  
19  
20  
21  
22  
23  
24  
25  
26  
27  
28  
29  
30  
31  
32  
33  
34

### 35 **MRSA cannot readily generate acute resistance to lead analogs.**

36  
37 After identifying which compounds selectively inhibited the GroEL chaperonin system  
38 and killed bacteria, we next evaluated whether bacteria could quickly develop resistance to lead  
39 candidate inhibitors. This was a concern we encountered with another series of GroEL/ES  
40 inhibitors we have been studying, represented by the bis-sulfonamido compound “**28R**” shown  
41 in **Figure 5**.<sup>38</sup> For this experiment, we adapted a liquid culture resistance assay from the  
42 previously established procedures of Kim *et al.*, and used our MRSA strain as the test bacteria (a  
43 detailed procedure is presented in the Supporting Information).<sup>38, 43</sup> Briefly, test compounds  
44 were incubated in dilution series with MRSA for 24 h and EC<sub>50</sub> values were determined. The  
45  
46  
47  
48  
49  
50  
51  
52  
53  
54  
55  
56  
57  
58  
59  
60

1  
2  
3 first well exhibiting OD<sub>600</sub> readings >0.2 were then sub-cultured for another 24 h with test  
4  
5 compound again in dilution series. Serial passage in this manner was conducted for a total of 12  
6  
7 days, and each day EC<sub>50</sub> values for the test compounds were determined: inhibitors to which  
8  
9 MRSA could rapidly generate resistance would exhibit increasing EC<sub>50</sub> results over each  
10  
11 successive passage. Rapid resistance was observed for the previously reported bis-sulfonamide  
12  
13 compound, **28R**, but was found to be reversible and likely owing to increased inhibitor efflux.<sup>38</sup>  
14  
15 We evaluated two of our lead GroEL inhibitors, **1** and **11**, along with vancomycin, and found  
16  
17 that all three exhibited exemplary antibiotic efficacy to which this MRSA strain was not able to  
18  
19 easily generate resistance.  
20  
21  
22  
23  
24  
25

### 26 **Compound 1 is bactericidal to *S. aureus* within established biofilms**

27  
28 While we found that *S. aureus* is not able to easily generate resistance to compounds **1**  
29  
30 and **11**, what remained to be seen was whether this series of inhibitors would be effective at  
31  
32 preventing bacteria from establishing biofilms and killing bacteria within already established  
33  
34 biofilms. Establishing biofilms is another effective mechanism by which *S. aureus* can evade the  
35  
36 effects of many current antibiotics, including vancomycin. To gauge the efficacy of lead  
37  
38 inhibitors at preventing *S. aureus* from forming biofilms, we employed an assay similar to the  
39  
40 liquid culture assay we used to determine inhibition of bacterial proliferation, with a few  
41  
42 modifications (detailed procedures presented in the Experimental section). Briefly, test  
43  
44 compounds (**1**, **2**, **5**, **8**, **11**, and vancomycin) were incubated with *S. aureus* bacteria in media  
45  
46 supplemented with 0.5% glucose (to support biofilm formation) for 24 h at 37°C. After 24 h, the  
47  
48 supernatant was removed, the wells were gently washed, and the biofilm that had formed on the  
49  
50 well surfaces were stained with crystal-violet and quantified by UV-Vis spectroscopy. We found  
51  
52  
53  
54  
55  
56  
57  
58  
59  
60

1  
2  
3 that all of the compound **1** analogs tested, and vancomycin, were able to prevent *S. aureus* from  
4 forming biofilms with EC<sub>50</sub> values nearly equipotent to antibacterial EC<sub>50</sub>s we determined  
5 against planktonic bacterial growth. Representative dose-response curves for compound **1** and  
6 vancomycin tested in these assays are presented in **Figure 6**, with a tabulation of test compound  
7 EC<sub>50</sub> results presented in **Table 4**. The high correlation of these results was not entirely  
8 surprising as compound **1** and vancomycin are bactericidal against *S. aureus*, and thus dead  
9 bacteria would not be able to form biofilms.<sup>31</sup>

19 Next, we evaluated whether or not compounds would be bactericidal to *S. aureus* that  
20 were within already established biofilms. In this assay, we first grew *S. aureus* bacteria for 24 h  
21 in the absence of test compounds so that they could establish biofilms in the wells. After 24 h,  
22 the cultures were removed, the wells were washed gently, and fresh media was added along with  
23 test compounds or vancomycin. The cultures were incubated in the presence of test compounds  
24 for another 24 h, then the wells were gently washed again to remove compounds and any  
25 planktonic bacteria that had emerged. Fresh media was then added and the cultures were  
26 incubated for another 24 h to allow any viable bacteria remaining in the biofilms to emerge and  
27 grow planktonically again. While there were 5-15-fold shifts in EC<sub>50</sub> values for the compound **1**  
28 analogs killing planktonic vs. biofilm bacteria (**Figure 6** and **Table 4**), these are still exciting  
29 results considering vancomycin was completely ineffective against biofilm bacteria (EC<sub>50</sub> >100  
30 μM), and especially since this class of GroEL/ES inhibitors has yet to be fully optimized. Thus,  
31 this scaffold shows considerable promise to take forward for further development as an  
32 antibacterial candidate.

## 33 CONCLUSIONS

1  
2  
3 In the present study, we developed a series of analogs of the previously identified hit  
4 GroEL inhibitor, compound **1**, and employed a molecular deconstruction strategy to  
5 systematically evaluate the contributions that the **R**<sup>1</sup> to **R**<sup>5</sup> substituents and substructures make  
6 towards selectively inhibiting the GroEL/ES chaperonin system and killing bacteria. We found  
7 that the benzothiazole **R**<sup>1</sup> group and hydroxyl **R**<sup>2</sup> substituent were integral to inhibiting  
8 GroEL/ES *in vitro*, but that the hydroxyl was the key determinant for being able to potently  
9 inhibit *S. aureus* proliferation. While trends are noted between IC<sub>50</sub> values from the GroEL/ES-  
10 dMDH refolding assay and the *E. faecium* and *S. aureus* proliferation assays, further experiments  
11 are warranted to conclusively determine whether or not inhibitors are on-target in bacteria.  
12 While some inhibitors were equipotent in the human HSP60/10-dMDH refolding assay, several  
13 exhibited only moderate to low cytotoxicity to liver and kidney cells. Importantly, compounds **1**  
14 and **11** did not encounter acute resistance through a 12-day serial passage in MRSA, generally  
15 maintaining efficacy <1 μM. Furthermore, compound **1** analogs were effective at killing *S.*  
16 *aureus* bacteria within established biofilms, whereas vancomycin was ineffective. These  
17 exemplary results support future med-chem derivatization efforts to optimize the *in vitro* and *in*  
18 *vivo* pharmacological properties of this class of GroEL/ES inhibitors for antibacterial  
19 development.

## 20 21 22 23 24 25 26 27 28 29 30 31 32 33 34 35 36 37 38 39 40 41 42 43 44 **EXPERIMENTAL**

### 45 46 47 **General Synthetic Methods.**

48  
49 Unless otherwise stated, all chemicals were purchased from commercial suppliers and  
50 used without further purification. Reaction progress was monitored by thin-layer  
51 chromatography on silica gel 60 F254 coated glass plates (EM Sciences). Flash chromatography  
52  
53  
54  
55  
56  
57  
58  
59  
60

1  
2  
3 was performed using a Biotage Isolera One flash chromatography system with elution through  
4 Biotage KP-Sil Zip or Snap silica gel columns for normal-phase separations (hexanes:EtOAc  
5 gradients) or Snap KP-C18-HS columns for reverse-phase separations (H<sub>2</sub>O:MeOH gradients).  
6  
7 Reverse-phase high-performance liquid chromatography (RP-HPLC) was performed using a  
8 Waters 1525 binary pump, 2489 tunable UV/Vis detector (254 and 280 nm detection), and 2707  
9  
10 autosampler. For preparatory HPLC purification, samples were chromatographically separated  
11 using a Waters XSelect CSH C18 OBD prep column (part number 186005422, 130 Å pore size,  
12 5 µm particle size, 19x150 mm), eluting with a H<sub>2</sub>O:CH<sub>3</sub>CN gradient solvent system. Linear  
13  
14 gradients were run from either 100:0, 80:20, or 60:40 A:B to 0:100 A:B (A = 95:5 H<sub>2</sub>O:CH<sub>3</sub>CN,  
15  
16 0.05% TFA; B = 5:95 H<sub>2</sub>O:CH<sub>3</sub>CN, 0.05% TFA. Products from normal-phase separations were  
17  
18 concentrated directly, and reverse-phase separations were concentrated, diluted with H<sub>2</sub>O,  
19  
20 frozen, and lyophilized. For primary compound purity analyses (HPLC-1), samples were  
21  
22 chromatographically separated using a Waters XSelect CSH C18 column (part number  
23  
24 186005282, 130 Å pore size, 5 µm particle size, 3.0x150 mm), eluting with the above  
25  
26 H<sub>2</sub>O:CH<sub>3</sub>CN gradient solvent systems. For secondary purity analyses (HPLC-2) of final test  
27  
28 compounds, samples were chromatographically separated using a Waters XBridge C18 column  
29  
30 (either part number 186003027, 130 Å pore size, 3.5 µm particle size, 3.0x100 mm, or part  
31  
32 number 186003132, 130 Å pore size, 5.0 µm particle size, 3.0x100 mm), eluting with a  
33  
34 H<sub>2</sub>O:MeOH gradient solvent system. Linear gradients were run from either 100:0, 80:20, 60:40,  
35  
36 or 20:80 A:B to 0:100 A:B (A = 95:5 H<sub>2</sub>O:MeOH, 0.05% TFA; B = 5:95 H<sub>2</sub>O:MeOH, 0.05%  
37  
38 TFA). Test compounds were found to be >95% pure from both RP-HPLC analyses. Mass  
39  
40 spectrometry data were collected using either an Agilent analytical LC-MS at the IU Chemical  
41  
42 Genomics Core Facility (CGCF), or a Thermo-Finnigan LTQ LC-MS in-lab. <sup>1</sup>H-NMR spectra  
43  
44  
45  
46  
47  
48  
49  
50  
51  
52  
53  
54  
55  
56  
57  
58  
59  
60



1  
2  
3 were recorded on a Bruker 300 MHz spectrometer at the CGCF. Chemical shifts are reported in  
4 parts per million and calibrated to the  $d_6$ -DMSO solvent peaks at 2.50 ppm. Synthesis and  
5  
6 characterization of intermediates **45-49** are presented below. General amide coupling and  
7  
8 methoxy deprotection steps are presented as follows using compounds **29** and **1** as representative  
9  
10 examples. Specific synthetic procedures and compound characterizations are presented in the  
11  
12 Supporting Information for the remaining analogs.  
13  
14  
15  
16  
17  
18

19 **45: 2-((2-Chloro-4-nitrophenyl)thio)benzo[*d*]thiazole.** 2-Mercaptobenzothiazole (11.9 g, 71.1  
20 mmol), 3,4-dichloronitrobenzene (11.8 g, 61.5 mmol), and potassium carbonate (11.7 g, 84.7  
21 mmol) were stirred together in DMF (60 mL) at R.T. overnight, then at 80°C for 4 h. The  
22  
23 reaction was then diluted with water and the precipitate was filtered, rinsed with water, and dried  
24  
25 to afford **45** as a yellow powder (19.5 g, 98% yield). <sup>1</sup>H-NMR (300 MHz,  $d_6$ -DMSO)  $\delta$  8.51 (d,  
26  
27  $J = 2.4$  Hz, 1H), 8.23 (dd,  $J = 8.7, 2.5$  Hz, 1H), 8.10 (d,  $J = 7.8$  Hz, 1H), 8.07-8.13 (m, 1H), 7.91  
28  
29 (d,  $J = 8.7$  Hz, 1H), 7.44-7.59 (m, 2H); MS (ESI) C<sub>13</sub>H<sub>8</sub>ClN<sub>2</sub>O<sub>2</sub>S<sub>2</sub> [MH]<sup>+</sup>  $m/z$  expected = 323.0,  
30  
31 observed = 323.1; HPLC-1 = 98%.  
32  
33  
34  
35  
36  
37  
38  
39

40 **46: 4-(Benzo[*d*]thiazol-2-ylthio)-3-chloroaniline.** Tin powder (5.64 g, 47.5 mmol) was added  
41  
42 slowly to a stirring mixture of **45** in a 1:10 mixture of HCl:AcOH (15 mL). The reaction was  
43  
44 allowed to stir at R.T. for 2 days, then diluted with EtOAc and H<sub>2</sub>O, neutralized with NaHCO<sub>3</sub>,  
45  
46 and filtered. The filtrate was extracted with EtOAc and the organics dried over Na<sub>2</sub>SO<sub>4</sub>, filtered,  
47  
48 and concentrated. The crude product was then chromatographed over silica (hexanes:EtOAc  
49  
50 gradient) and concentrated. The residue was diluted in a 4:1 mixture of hexanes:DCM and the  
51  
52 precipitate was filtered and dried to afford **46** as a yellow powder (3.73 g, 81% yield). <sup>1</sup>H-NMR  
53  
54  
55  
56  
57  
58  
59  
60

1  
2  
3 (300 MHz,  $d_6$ -DMSO)  $\delta$  7.87-7.96 (m, 1H), 7.80 (d,  $J$  = 8.1 Hz, 1H), 7.53 (d,  $J$  = 8.5 Hz, 1H),  
4  
5 7.43 (td,  $J$  = 7.7, 1.3 Hz, 1H), 7.26-7.34 (m, 1H), 6.87 (d,  $J$  = 2.4 Hz, 1H), 6.64 (dd,  $J$  = 8.5, 2.4  
6  
7 Hz, 1H), 6.18 (s, 2H); MS (ESI)  $C_{13}H_{10}ClN_2S_2$   $[MH]^+$   $m/z$  expected = 293.0, observed = 293.0;  
8  
9 HPLC-1 = 98%.

10  
11  
12  
13  
14 **47: 4-(Benzo[*d*]thiazol-2-ylthio)aniline.** 2-Chlorobenzothiazole (2.00 g, 11.8 mmol), 4-  
15  
16 aminothiophenol (1.70 g, 13.6 mmol), and potassium carbonate (3.24 g, 23.4 mmol) were stirred  
17  
18 together in EtOH (15 mL) for 18 h. The reaction was then diluted with water and the precipitate  
19  
20 was filtered, rinsed with water, and collected. Flash chromatographic purification  
21  
22 (hexanes:EtOAc gradient) afforded **47** as an off-white solid (2.71 g, 89% yield).  $^1H$ -NMR (300  
23  
24 MHz,  $d_6$ -DMSO)  $\delta$  7.85-7.91 (m, 1H), 7.78 (d,  $J$  = 7.7 Hz, 1H), 7.37-7.45 (m, 3H), 7.25-7.34 (m,  
25  
26 1H), 6.66-6.73 (m, 2H), 5.84 (s, 1H); MS (ESI)  $C_{13}H_{11}N_2S_2$   $[MH]^+$   $m/z$  expected = 259.0,  
27  
28 observed = 259.0; HPLC-1 = >99%.

29  
30  
31  
32  
33  
34  
35 **48: 3,5-Dibromo-2-methoxybenzoic acid.** Iodomethane (6.30 mL, 101 mmol), 3,5-  
36  
37 dibromosalicylic acid (10.0 g, 33.7 mmol), and  $K_2CO_3$  (14.0 g, 101 mmol) were stirred at R.T.  
38  
39 overnight, then at 80°C for 4 h. The reaction was diluted into water and extracted into DCM.  
40  
41 The organics were dried over  $Na_2SO_4$ , filtered, and concentrated. The intermediate ester was  
42  
43 then stirred overnight with  $LiOH \cdot H_2O$  (5.70 g, 136 mmol) in a 3:1:1 mixture of  
44  
45 THF:MeOH:H<sub>2</sub>O (35 mL). The reaction was diluted with water and acidified with HCl. The  
46  
47 precipitate was filtered, washed with water, and dried to afford **48** as a white solid (9.85 g, 94%  
48  
49 yield).  $^1H$ -NMR (300 MHz,  $d_6$ -DMSO)  $\delta$  13.56 (br s, 1H), 8.09 (d,  $J$  = 2.5 Hz, 1H), 7.83 (d,  $J$  =  
50  
51  
52  
53  
54  
55  
56  
57  
58  
59  
60

2.5 Hz, 1H), 3.81 (s, 3H); MS (ESI)  $C_8H_5Br_2O_3$   $[M-H]^-$   $m/z$  expected = 308.9, observed = 309.1; HPLC-1 = >99%.

**49: 5-Bromo-2-methoxybenzoic acid.** 5-Bromosalicylic acid (10.0 g, 46.1 mmol), iodomethane (8.60 mL, 138 mmol), and  $K_2CO_3$  (19.0 g, 137 mmol) were stirred at R.T. overnight, then at 80°C for 4 h. The reaction was diluted into water and the precipitate was filtered, rinsed with water, and dried. The intermediate ester was then stirred overnight with  $LiOH \cdot H_2O$  (7.70 g, 184 mmol) in a 3:1:1 mixture of THF:MeOH:H<sub>2</sub>O (45 mL). The reaction was diluted with water and acidified with HCl. The precipitate was filtered, washed with water, and dried to afford **49** as a white solid (8.70 g, 82% yield). <sup>1</sup>H-NMR (300 MHz, *d*<sub>6</sub>-DMSO)  $\delta$  12.98 (br s, 1H), 7.72 (d, *J* = 2.6 Hz, 1H), 7.66 (dd, *J* = 8.8, 2.6 Hz, 1H), 7.10 (d, *J* = 8.9 Hz, 1H), 3.81 (s, 3H); MS (ESI)  $C_8H_6BrO_3$   $[M-H]^-$   $m/z$  expected = 229.0, observed = 229.0; HPLC-1 = 98%.

### General procedure for the amide coupling step using analog **29** as a representative

#### example: *N*-(4-(Benzo[*d*]thiazol-2-ylthio)-3-chlorophenyl)-3,5-dibromo-2-

**methoxybenzamide.** Compound **48** (225 mg, 0.726 mmol) was stirred in  $SOCl_2$  (2 mL) at 60°C for 1 h, then was concentrated. Anhydrous DCM (5 mL), compound **46** (148 mg, 0.505 mmol), and pyridine (62.0  $\mu$ L, 0.760 mmol) were added and the reaction was stirred at R.T. for 18 h (under Ar). Flash chromatographic purification (hexanes:EtOAc gradient) afforded **29** as a yellow solid (58.6 mg, 20% yield). <sup>1</sup>H-NMR (300 MHz, *d*<sub>6</sub>-DMSO)  $\delta$  11.00 (s, 1H), 8.21 (d, *J* = 2.1 Hz, 1H), 8.10 (d, *J* = 2.3 Hz, 1H), 7.97 (t, *J* = 8.3 Hz, 2H), 7.82-7.87 (m, 2H), 7.78 (dd, *J* = 8.6, 2.2 Hz, 1H), 7.47 (td, *J* = 7.7, 1.3 Hz, 1H), 7.32-7.38 (m, 1H), 3.84 (s, 3H); MS (ESI)

1  
2  
3  $C_{21}H_{12}Br_2ClN_2O_2S_2$  [M-H]<sup>-</sup> *m/z* expected = 580.8, observed = 580.7; HPLC-1 = >99%; HPLC-2  
4  
5 = >99%.  
6  
7  
8  
9

10 **General procedure for the methoxy deprotection step to give hydroxylated compounds**  
11 **using analog 1 as a representative example: *N*-(4-(Benzo[*d*]thiazol-2-ylthio)-3-**

12 **chlorophenyl)-3,5-dibromo-2-hydroxybenzamide.** To a stirring mixture of **29** (51.0 mg,  
13  
14 0.0872 mmol) in anhydrous DCM (5 mL) was added BBr<sub>3</sub> (0.26 mL of 1 M in DCM, 0.26  
15  
16 mmol). The reaction was allowed to stir at R.T. (under Ar) for 18 h and then quenched with  
17  
18 MeOH. Flash chromatographic purification (hexanes:EtOAc gradient) afforded **1** as an off-white  
19  
20 solid (34.4 mg, 69% yield). <sup>1</sup>H-NMR (300 MHz, *d*<sub>6</sub>-DMSO) δ 11.14 (br s, 1H), 8.19 (dd, *J*=  
21  
22 6.2, 2.2 Hz, 2H), 7.94-8.05 (m, 3H), 7.82-7.89 (m, 2H), 7.47 (td, *J* = 7.7, 1.3 Hz, 1H), 7.33-7.40  
23  
24 (m, 1H); MS (ESI)  $C_{20}H_{10}Br_2ClN_2O_2S_2$  [M-H]<sup>-</sup> *m/z* expected = 566.8, observed = 566.6; HPLC-1  
25  
26 = 99%; HPLC-2 = 98%.  
27  
28  
29  
30  
31  
32  
33  
34

35 **Protein Expression and purification.**

36  
37 *E. coli* GroEL and GroES, and human HSP60 and HSP10, were expressed and purified as  
38  
39 previously reported.<sup>30, 31, 38, 40, 44</sup> Detailed protocols for these protein purifications are presented  
40  
41 in the Supporting Information.  
42  
43  
44  
45  
46

47 **Control compounds for assays.**

48  
49 For all of the biochemical assays (GroEL/ES and HSP60/10-mediated dMDH and dRho  
50  
51 refolding assays, and native MDH and Rho enzymatic activity counter-screens), DMSO was  
52  
53 used as negative control, and a panel of our previously discovered and reported chaperonin  
54  
55  
56  
57  
58  
59  
60

1  
2  
3 inhibitors were used as positive controls: e.g. compound **1** herein; compounds **9** and **18** from  
4 Johnson *et. al* 2014 and Abdeen *et. al* 2016<sup>30, 31</sup>; suramin and compound **2h-p** from Abdeen *et. al*  
5 2016<sup>40</sup>; and compounds **20R**, **20L**, and **28R** from Abdeen *et. al* 2018.<sup>38</sup> For the bacterial  
6 proliferation assays, control compounds included the aforementioned panel of previously  
7 reported chaperonin inhibitors as well as vancomycin, daptomycin, ampicillin, and rifampicin.  
8 For the human cell viability assays, control compounds include the aforementioned compounds  
9 as well as other protein homeostasis inhibitors, such as bortezomib (proteasome inhibitor); VER-  
10 155008 (HSP70 inhibitor); and ganetespib and 17-DMAG (HSP90 inhibitors).  
11  
12  
13  
14  
15  
16  
17  
18  
19  
20  
21  
22  
23

#### 24 **Evaluation of compounds in GroEL/ES and HSP60/10-mediated dMDH and dRho** 25 **refolding assays.**

26  
27 All compounds were evaluated for inhibiting *E. coli* GroEL/ES and human HSP60/10-  
28 mediated refolding of the denatured MDH and denatured Rho reporter enzymes as per previously  
29 reported procedures.<sup>30, 31, 38, 40</sup> Detailed protocols for these assays are presented in the  
30 Supporting Information.  
31  
32  
33  
34  
35  
36  
37  
38  
39

#### 40 **Counter-screening compounds for inhibition of native MDH and Rho enzymatic activity.**

41  
42 All compounds were counter-screened for inhibiting the enzymatic activity of the native  
43 MDH and native Rho reporter enzymes as per previously reported procedures.<sup>30, 31, 38, 40</sup> Detailed  
44 protocols for the assays are presented in the Supporting Information.  
45  
46  
47  
48  
49  
50

#### 51 **Cell information for compound evaluation.**

52  
53  
54  
55  
56  
57  
58  
59  
60

1  
2  
3 The *ESKAPE* bacteria were purchased from the American Type Culture Collection  
4 (ATCC): *E. faecium* (Orla-Jensen) Schleifer and Kilpper-Balz strain NCTC 7171 (ATCC  
5 19434); *S. aureus* subsp. *aureus* Rosenbach strain Seattle 1945 (ATCC 25923); Multi-drug  
6 resistant *S. aureus* (MRSA) subsp. *aureus* Rosenbach strain HPV107 (ATCC BAA-44); *K.*  
7 *pneumoniae*, subsp. *pneumoniae* (Schroeter) Trevisan strain NCTC 9633 (ATCC 13883); *A.*  
8 *baumannii* Bouvet and Grimont strain 2208 (ATCC 19606); *P. aeruginosa* (Schroeter) Migula  
9 strain NCTC 10332 (ATCC 10145); *E. cloacae*, subsp. *cloacae* (Jordan) Hormaeche and  
10 Edwards strain CDC 442-68 (ATCC 13047). Human THLE-3 liver cells (ATCC CRL-11233)  
11 and HEK 293 kidney cells (ATCC CRL-1573) were used for the cell viability assays.  
12  
13  
14  
15  
16  
17  
18  
19  
20  
21  
22  
23  
24  
25

#### 26 **Evaluation of compounds for inhibition of bacterial cell proliferation.**

27  
28 All compounds were evaluated for inhibiting the proliferation of each of the *ESKAPE*  
29 bacteria as per previously reported procedures.<sup>38</sup> Detailed protocols for bacterial growth assays  
30 are presented in the Supporting Information.  
31  
32  
33  
34  
35  
36  
37

#### 38 **Evaluation of compound effects on HEK 293 and THLE-3 cell viability.**

39  
40 All compounds were evaluated for cytotoxicities to THLE-3 liver and HEK 293 kidney  
41 cells using Alamar Blue-based viability assays as per previously reported procedures.<sup>31, 38, 40</sup>  
42 Detailed protocols for these assays are presented in the Supporting Information.  
43  
44  
45  
46  
47  
48

#### 49 **Evaluation of MRSA resistance generation against lead inhibitors.**

50  
51 To identify potential resistance toward compounds **1** and **11**, a liquid culture, 12-day  
52 serial passage assay was employed as per previously reported procedures, and using the ATCC  
53  
54  
55  
56  
57  
58  
59  
60

1  
2  
3 BAA-44 MRSA strain.<sup>38, 43, 45</sup> A detailed protocol for this assay is presented in the Supporting  
4  
5 Information.  
6  
7  
8  
9

### 10 ***S. aureus* Biofilm Prevention Assay.**

11  
12 The biofilm prevention assay was carried out with *S. aureus* Rosenbach (ATCC 25923)  
13 using a quantitative crystal violet-based adherence assay on 96-well plates as described  
14 previously by Kwasny *et al.*<sup>46</sup> *S. aureus* (ATCC 25923) bacteria were streaked onto a Tryptic  
15 Soy Broth (TSB) agar plate and grown overnight at 37°C. A fresh aliquot of TSB media was  
16 inoculated with a single bacterial colony and the cultures were grown overnight at 37°C with  
17 shaking (250 rpm). The overnight culture was then sub-cultured (1:5 dilution) into a fresh  
18 aliquot of TSB media supplemented to a final concentration of 0.5% glucose and grown at 37°C  
19 for 1 h with shaking, then diluted into fresh TSB media supplemented with 0.5% glucose to  
20 achieve a final OD<sub>600</sub> reading of 0.01. Aliquots of the diluted culture (100 µL) were dispensed to  
21 96 well polystyrene plates along with addition of 1 µL test compounds in DMSO. The inhibitor  
22 concentration range during the assay was 100 µM to 46 nM (3-fold dilution series). A second set  
23 of baseline control plates were prepared analogously, but without any bacteria added, to correct  
24 for possible compound absorbance and/or precipitation. Plates were sealed with "Breathe Easy"  
25 oxygen permeable membranes (Diversified Biotech) and left to incubate at 37°C without shaking  
26 (stagnant assay) until the biofilm was formed. After 24 h, the planktonic cultures were removed  
27 and the plates were washed gently 2-3 times with 200 µl of water. Next, the plates were air dried  
28 and the adherent biofilms were stained with 150 µL of crystal violet solution (2.3% crystal violet  
29 in 20% Ethanol, Sigma Aldrich #HT90132) for 15 minutes at R.T. The unbound crystal violet  
30 stain was removed, then plates were gently washed again with running water and air dried for 10  
31  
32  
33  
34  
35  
36  
37  
38  
39  
40  
41  
42  
43  
44  
45  
46  
47  
48  
49  
50  
51  
52  
53  
54  
55  
56  
57  
58  
59  
60

1  
2  
3 min. Quantitative assessment of biofilm formation was obtained by adding 100  $\mu$ L of developer  
4 solution (4:1:5 mixture of MeOH:AcOH:H<sub>2</sub>O) per well. Well absorbance was then read at 595  
5 nm using a Molecular Devices SpectraMax Plus384 microplate reader. EC<sub>50</sub> values for the test  
6  
7  
8 compounds were obtained by plotting the A<sub>595 nm</sub> results in GraphPad Prism 6 and analyzing by  
9  
10 non-linear regression using the log(inhibitor) vs. response (variable slope) equation. Results  
11  
12 presented represent the averages of EC<sub>50</sub> values obtained from at least triplicate experiments.  
13  
14  
15  
16  
17  
18

### 19 ***S. aureus* Biofilm Penetration and Bactericidal Activity Assay.**

20  
21 The biofilm penetration and bactericidal activity assay was carried out with *S. aureus*  
22 Rosenbach (ATCC 25923) as described previously by Kwasny *et al.*<sup>46</sup> *S. aureus* bacteria were  
23 streaked onto a Tryptic Soy Broth (TSB) agar plate and grown overnight at 37°C. A fresh  
24 aliquot of TSB media was inoculated with a single bacterial colony and the cultures were grown  
25 overnight at 37°C with shaking (250 rpm). The overnight culture was then sub-cultured (1:5  
26 dilution) into a fresh aliquot of TSB media supplemented with 0.5% glucose and grown at 37°C  
27 for 1 h with shaking, then diluted into fresh TSB media supplemented with 0.5% glucose to  
28 achieve a final OD<sub>600</sub> reading of 0.01. Aliquots of the diluted culture (100  $\mu$ L) were dispensed to  
29 96 well polystyrene plates without any compounds added. A second set of control plates were  
30 prepared analogously, but without any bacteria added. Plates were sealed with "Breathe Easy"  
31 oxygen permeable membranes (Diversified Biotech) and left to incubate at 37°C without shaking  
32 (stagnant assay) until biofilm was formed. After 24 h, the planktonic cultures (or media blanks  
33 in the control plates) were removed and the plates were washed gently 3 times with 200  $\mu$ L of  
34 sterile phosphate buffered saline (PBS). Then, 100  $\mu$ L aliquots of fresh TSB media were  
35 dispensed to the plates along with addition of 1  $\mu$ L of test compounds in DMSO. The inhibitor  
36  
37  
38  
39  
40  
41  
42  
43  
44  
45  
46  
47  
48  
49  
50  
51  
52  
53  
54  
55  
56  
57  
58  
59  
60



1  
2  
3 concentration range during the assay was 100  $\mu\text{M}$  to 46 nM (3-fold dilution series). The plates  
4 were sealed with "Breathe Easy" membranes and incubated at 37°C without shaking to allow  
5  
6 compounds to penetrate and kill bacteria in the biofilms. After 24 h, the cultures were removed  
7  
8 and plates were washed again gently 3 times with 200  $\mu\text{L}$  of sterile PBS. The remaining bacteria  
9  
10 in the biofilms were allowed to recover by adding 100  $\mu\text{L}$  of fresh TSB media per well and  
11  
12 incubating for 24 h at 37°C. At the end of this final incubation, bacterial growth was monitored  
13  
14 by measuring the  $\text{OD}_{600\text{ nm}}$  using a Molecular Devices SpectraMax Plus384 microplate reader.  
15  
16  $\text{EC}_{50}$  values for the test compounds were obtained by plotting the  $\text{OD}_{600\text{ nm}}$  results in GraphPad  
17  
18 Prism 6 and analyzing by non-linear regression using the log(inhibitor) vs. response (variable  
19  
20 slope) equation. Results presented represent the averages of  $\text{EC}_{50}$  values obtained from at least  
21  
22 triplicate experiments.  
23  
24  
25  
26  
27  
28  
29  
30

### 31 **Calculation of $\text{IC}_{50}$ / $\text{EC}_{50}$ / $\text{CC}_{50}$ values and statistical considerations.**

32  
33 All  $\text{IC}_{50}$  /  $\text{EC}_{50}$  /  $\text{CC}_{50}$  results reported are averages of values determined from individual  
34  
35 dose-response curves in assay replicates as follows: 1) Individual I/E/ $\text{CC}_{50}$  values from assay  
36  
37 replicates were first log-transformed and the average log(I/E/ $\text{CC}_{50}$ ) values and standard  
38  
39 deviations (SD) calculated; 2) Replicate log(I/E/ $\text{CC}_{50}$ ) values were evaluated for outliers using  
40  
41 the ROUT method in GraphPad Prism 6 (Q of 10%); and 3) Average I/E/ $\text{CC}_{50}$  values were then  
42  
43 back-calculated from the average log(I/E/ $\text{CC}_{50}$ ) values. To compare log(I/E/ $\text{CC}_{50}$ ) values  
44  
45 between different assays, two-tailed Spearman correlation analyses were performed using  
46  
47 GraphPad Prism 6 (95% confidence level). For compounds where log(I/E/ $\text{CC}_{50}$ ) values were  
48  
49 greater than the maximum compound concentrations tested (i.e. >2.0, or >100  $\mu\text{M}$ ), results were  
50  
51 represented as 0.1 log units higher than the maximum concentrations tested (i.e. 2.1, or 126  $\mu\text{M}$ ),  
52  
53  
54  
55  
56  
57  
58  
59  
60

1  
2  
3 so as not to overly bias comparisons because of the unavailability of definitive values for these  
4  
5 inactive compounds.  
6  
7  
8  
9

### 10 **Corresponding Author**

11  
12 \* E-mail: johnstm@iu.edu, Phone: 317-274-2458, Fax: 317-274-4686.  
13  
14  
15

### 16 **ACKNOWLEDGMENTS**

17  
18  
19 Research reported in this publication was supported by the National Institute of General Medical  
20  
21 Sciences (NIGMS) of the National Institutes of Health (NIH) under Award Number  
22  
23 R01GM120350. QQH and YP additionally acknowledge support by NIH grants  
24  
25 5R01GM111639 and 5R01GM115844. The content is solely the responsibility of the authors  
26  
27 and does not necessarily represent the official views of the NIH. This work was also supported  
28  
29 in part by startup funds from the IU School of Medicine (SMJ) and the University of Arizona  
30  
31 (EC). The human HSP60 expression plasmid (lacking the 26 amino acid *N*-terminal  
32  
33 mitochondrial signal peptide) was generously donated by Dr. Abdussalam Azem from Tel Aviv  
34  
35 University, Faculty of Life Sciences, Department of Biochemistry, Israel.  
36  
37  
38  
39  
40  
41

### 42 **ABBREVIATIONS**

43  
44 MDH, malate dehydrogenase; Rho, rhodanese; IC<sub>50</sub> - Inhibitory concentration for half-maximal  
45  
46 signal in biochemical assay; EC<sub>50</sub>, effective concentration for half-maximal signal in bacterial  
47  
48 proliferation assays; CC<sub>50</sub>, cytotoxicity concentration for half-maximal signal in human cell  
49  
50 viability assays.  
51  
52  
53  
54  
55  
56  
57  
58  
59  
60

**SUPPORTING INFORMATION**

Supporting Information associated with this article can be found in the online version, which includes tabulation of all  $\log(\text{IC}_{50})$ ,  $\log(\text{EC}_{50})$ , and  $\log(\text{CC}_{50})$  results with standard deviations; synthetic protocols and characterization data for test compounds (MS,  $^1\text{H-NMR}$ , and HPLC purity); experimental protocols for protein synthesis and purification, and biochemical, bacterial proliferation, and human cell viability assays; and SMILES strings of compound structures.

## REFERENCES

1. Centers for Disease Control and Prevention. *Antibiotic resistance threats in the United States, 2013*. Centers for Disease Control and Prevention: Atlanta, Georgia, USA, 2013; p 114.
2. Boucher, H. W.; Talbot, G. H.; Bradley, J. S.; Edwards, J. E.; Gilbert, D.; Rice, L. B.; Scheld, M.; Spellberg, B.; Bartlett, J. Bad bugs, no drugs: No ESCAPE! An update from the Infectious Diseases Society of America. *Clin. Infect. Dis.* **2009**, 48, 1-12.
3. Lewis, K. Platforms for antibiotic discovery. *Nat. Rev. Drug Discov.* **2013**, 12, 371-387.
4. Wright, G. D.; Sutherland, A. D. New strategies for combating multidrug-resistant bacteria. *Trends Mol. Med.* **2007**, 13, 260-267.
5. Bjarnsholt, T. The role of bacterial biofilms in chronic infections. *APMIS Suppl.* **2013**, 1-51.
6. Stewart, P. S.; Costerton, J. W. Antibiotic resistance of bacteria in biofilms. *Lancet* **2001**, 358, 135-138.
7. Singh, R.; Ray, P.; Das, A.; Sharma, M. Penetration of antibiotics through *Staphylococcus aureus* and *Staphylococcus epidermidis* biofilms. *J. Antimicrob. Chemother.* **2010**, 65, 1955-1958.
8. Hartl, F. U.; Bracher, A.; Hayer-Hartl, M. Molecular chaperones in protein folding and proteostasis. *Nature* **2011**, 475, 324-332.
9. Stefani, M.; Dobson, C. M. Protein aggregation and aggregate toxicity: new insights into protein folding, misfolding diseases and biological evolution. *J. Mol. Med. (Berl.)* **2003**, 81, 678-699.
10. Maisonneuve, E.; Ezraty, B.; Dukan, S. Protein aggregates: An aging factor involved in cell death. *J. Bacter.* **2008**, 190, 6070-6075.

- 1  
2  
3 11. Carmichael, J.; Chatellier, J.; Woolfson, A.; Milstein, C.; Fersht, A. R.; Rubinsztein, D. C.  
4  
5 Bacterial and yeast chaperones reduce both aggregate formation and cell death in  
6  
7 mammalian cell models of Huntington's disease. *Proc. Natl. Acad. Sci. U.S.A.* **2000**, *97*,  
8  
9 9701-9705.  
10  
11
- 12 12. Bao, Y. P.; Cook, L. J.; O'Donovan, D.; Uyama, E.; Rubinsztein, D. C. Mammalian, yeast,  
13  
14 bacterial, and chemical chaperones reduce aggregate formation and death in a cell model of  
15  
16 oculopharyngeal muscular dystrophy. *J. Biol. Chem.* **2002**, *277*, 12263-12269.  
17  
18
- 19 13. Park, H. K.; Lee, J. E.; Lim, J.; Jo, D. E.; Park, S. A.; Suh, P. G.; Kang, B. H. Combination  
20  
21 treatment with doxorubicin and gamitrinib synergistically augments anticancer activity  
22  
23 through enhanced activation of Bim. *BMC Cancer* **2014**, *14*, 431.  
24  
25
- 26 14. Whitesell, L.; Lin, N. U. HSP90 as a platform for the assembly of more effective cancer  
27  
28 chemotherapy. *Biochim. Biophys. Acta Mol. Cell Res.* **2012**, *1823*, 756-766.  
29  
30
- 31 15. Whitesell, L.; Lindquist, S. L. HSP90 and the chaperoning of cancer. *Nat. Rev. Cancer*  
32  
33 **2005**, *5*, 761-772.  
34
- 35 16. Chiappori, F.; Fumian, M.; Milanesi, L.; Merelli, I. DnaK as antibiotic target: Hot spot  
36  
37 residues analysis for differential inhibition of the bacterial protein in comparison with the  
38  
39 human HSP70. *PLoS One* **2015**, *10*, e0124563.  
40  
41
- 42 17. Arita-Morioka, K.; Yamanaka, K.; Mizunoe, Y.; Ogura, T.; Sugimoto, S. Novel strategy for  
43  
44 biofilm inhibition by using small molecules targeting molecular chaperone DnaK.  
45  
46 *Antimicrob. Agents Chemother.* **2015**, *59*, 633-641.  
47  
48
- 49 18. Sass, P.; Josten, M.; Famulla, K.; Schiffer, G.; Sahl, H. G.; Hamoen, L.; Brotz-Oesterhelt,  
50  
51 H. Antibiotic acyldepsipeptides activate ClpP peptidase to degrade the cell division protein  
52  
53 FtsZ. *Proc. Natl. Acad. Sci. U.S.A.* **2011**, *108*, 17474-17479.  
54  
55  
56  
57  
58  
59  
60

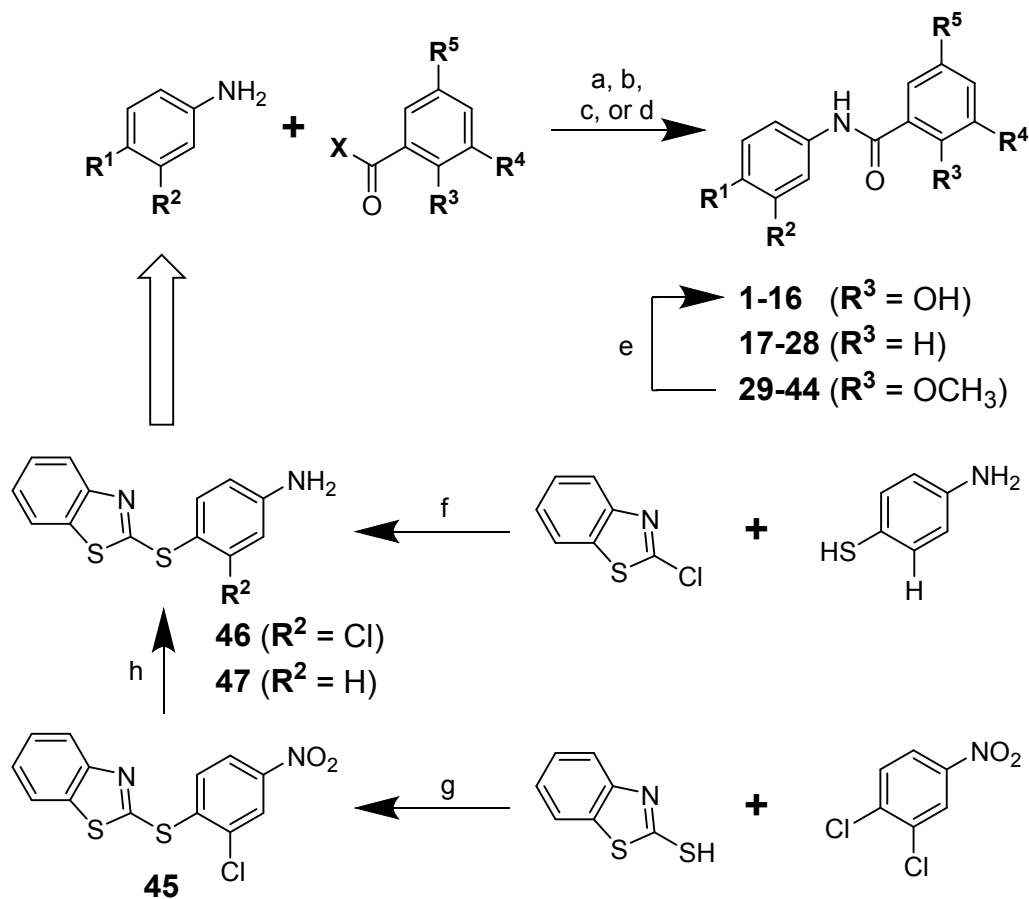
19. Evans, C. G.; Chang, L.; Gestwicki, J. E. Heat shock protein 70 (hsp70) as an emerging drug target. *J. Med. Chem.* **2010**, *53*, 4585-4602.
20. Piper, P. W.; Millson, S. H. Spotlight on the microbes that produce heat shock protein 90-targeting antibiotics. *Open Biology* **2012**, *2*, 120138.
21. Braig, K.; Otwinowski, Z.; Hegde, R.; Boisvert, D. C.; Joachimiak, A.; Horwich, A. L.; Sigler, P. B. The crystal structure of the bacterial chaperonin GroEL at 2.8 Å. *Nature* **1994**, *371*, 578-586.
22. Sigler, P. B.; Xu, Z.; Rye, H. S.; Burston, S. G.; Fenton, W. A.; Horwich, A. L. Structure and function in GroEL-mediated protein folding. *Annu. Rev. Biochem.* **1998**, *67*, 581-608.
23. Horwich, A. L.; Farr, G. W.; Fenton, W. A. GroEL-GroES-mediated protein folding. *Chem. Rev.* **2006**, *106*, 1917-1930.
24. Fenton, W. A.; Kashi, Y.; Furtak, K.; Horwich, A. L. Residues in chaperonin GroEL required for polypeptide binding and release. *Nature* **1994**, *371*, 614-619.
25. Fenton, W. A.; Horwich, A. L. GroEL-mediated protein folding. *Protein Sci.* **1997**, *6*, 743-760.
26. Horwich, A. L.; Fenton, W. A.; Chapman, E.; Farr, G. W. Two families of chaperonin: physiology and mechanism. *Annu. Rev. Cell. Dev. Biol.* **2007**, *23*, 115-145.
27. Saibil, H. R.; Fenton, W. A.; Clare, D. K.; Horwich, A. L. Structure and allostery of the chaperonin GroEL. *J. Mol. Biol.* **2013**, *425*, 1476-1487.
28. Chapman, E.; Farr, G. W.; Usaite, R.; Furtak, K.; Fenton, W. A.; Chaudhuri, T. K.; Hondorp, E. R.; Matthews, R. G.; Wolf, S. G.; Yates, J. R.; Pypaert, M.; Horwich, A. L. Global aggregation of newly translated proteins in an *Escherichia coli* strain deficient of the chaperonin GroEL. *Proc. Natl. Acad. Sci. U.S.A.* **2006**, *103*, 15800-15805.

- 1  
2  
3 29. Fayet, O.; Ziegelhoffer, T.; Georgopoulos, C. The groES and groEL heat shock gene  
4 products of Escherichia coli are essential for bacterial growth at all temperatures. *J.*  
5  
6  
7 *Bacteriol.* **1989**, 171, 1379-1385.  
8  
9
- 10 30. Johnson, S. M.; Sharif, O.; Mak, P. A.; Wang, H. T.; Engels, I. H.; Brinker, A.; Schultz, P.  
11 G.; Horwich, A. L.; Chapman, E. A biochemical screen for GroEL/GroES inhibitors.  
12  
13 *Bioorg. Med. Chem. Lett.* **2014**, 24, 786-789.  
14  
15  
16
- 17 31. Abdeen, S.; Salim, N.; Mammadova, N.; Summers, C. M.; Frankson, R.; Ambrose, A. J.;  
18 Anderson, G. G.; Schultz, P. G.; Horwich, A. L.; Chapman, E.; Johnson, S. M. GroEL/ES  
19 inhibitors as potential antibiotics. *Bioorg. Med. Chem. Lett.* **2016**, 26, 3127-3134.  
20  
21  
22
- 23 32. Safonova, T. V.; Fedyanina, L. V.; Trusov, S. N.; Feoktistova, T. S.; Sevbo, D. P.;  
24 Mikhailitsyn, F. S. Antitrichocephalous activity of the agents G-1730 and G-1732.  
25  
26 *Meditinskaya Parazitologiya i Parazitarnye Bolezni* **2003**, 21-22.  
27  
28  
29
- 30 33. Stromberg, B. E.; Schlotthauer, J. C.; Conboy, G. A. The efficacy of closantel against  
31 Fascioloides magna in sheep. *J. Parasitol.* **1984**, 70, 446-447.  
32  
33  
34
- 35 34. Cheng, T. J.; Wu, Y. T.; Yang, S. T.; Lo, K. H.; Chen, S. K.; Chen, Y. H.; Huang, W. I.;  
36 Yuan, C. H.; Guo, C. W.; Huang, L. Y.; Chen, K. T.; Shih, H. W.; Cheng, Y. S.; Cheng, W.  
37 C.; Wong, C. H. High-throughput identification of antibacterials against methicillin-resistant  
38 Staphylococcus aureus (MRSA) and the transglycosylase. *Bioorg. Med. Chem.* **2010**, 18,  
39 8512-8529.  
40  
41  
42
- 43 35. Johnson, S. M.; Connelly, S.; Wilson, I. A.; Kelly, J. W. Toward optimization of the linker  
44 substructure common to transthyretin amyloidogenesis inhibitors using biochemical and  
45 structural studies. *J. Med. Chem.* **2008**, 51, 6348-6358.  
46  
47  
48  
49  
50  
51  
52  
53  
54  
55  
56  
57  
58  
59  
60

- 1  
2  
3 36. Connelly, S.; Mortenson, D. E.; Choi, S.; Wilson, I. A.; Powers, E. T.; Kelly, J. W.;  
4  
5 Johnson, S. M. Semi-quantitative models for identifying potent and selective transthyretin  
6  
7 amyloidogenesis inhibitors. *Bioorg. Med. Chem. Lett.* **2017**, *27*, 3441-3449.  
8  
9  
10 37. Johnson, S. M.; Connelly, S.; Wilson, I. A.; Kelly, J. W. Toward optimization of the second  
11  
12 aryl substructure common to transthyretin amyloidogenesis inhibitors using biochemical and  
13  
14 structural studies. *J. Med. Chem.* **2009**, *52*, 1115-1125.  
15  
16  
17 38. Abdeen, S.; Kunkle, T.; Salim, N.; Ray, A. M.; Mammadova, N.; Summers, C.; Stevens,  
18  
19 M.; Ambrose, A. J.; Park, Y.; Schultz, P. G.; Horwich, A. L.; Hoang, Q. Q.; Chapman, E.;  
20  
21 Johnson, S. M. Sulfonamido-2-arylbenzoxazole GroEL/ES Inhibitors as Potent  
22  
23 Antibacterials against Methicillin-Resistant Staphylococcus aureus (MRSA). *J Med Chem*  
24  
25 **2018**, *61*, 7345-7357.  
26  
27  
28 39. Heinz, L. J.; Panetta, J. A.; Phillips, M. L.; Reel, J. K.; Shadle, J. K.; Simon, R. L.;  
29  
30 Whitesitt, C. A. Preparation of (Hetero)arylthioureas and Analogs as Amyloid  $\beta$ -protein  
31  
32 Biosynthesis Inhibitors. US 5814646, 1998.  
33  
34  
35 40. Abdeen, S.; Salim, N.; Mammadova, N.; Summers, C. M.; Goldsmith-Pestana, K.;  
36  
37 McMahon-Pratt, D.; Schultz, P. G.; Horwich, A. L.; Chapman, E.; Johnson, S. M. Targeting  
38  
39 the HSP60/10 chaperonin systems of *Trypanosoma brucei* as a strategy for treating African  
40  
41 sleeping sickness. *Bioorg. Med. Chem. Lett.* **2016**, *26*, 5247-5253.  
42  
43  
44 41. Martin, R. J. Modes of action of anthelmintic drugs. *Vet. J.* **1997**, *154*, 11-34.  
45  
46  
47 42. Martin, R. J.; Robertson, A. P.; Bjorn, H. Target sites of anthelmintics. *Parasitology* **1997**,  
48  
49 *114*, S111-S124.  
50  
51  
52  
53  
54  
55  
56  
57  
58  
59  
60

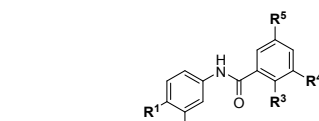


- 1  
2  
3 43. Kim, S.; Lieberman, T. D.; Kishony, R. Alternating antibiotic treatments constrain  
4  
5 evolutionary paths to multidrug resistance. *Proc. Natl. Acad. Sci. U.S.A.* **2014**, 111, 14494-  
6  
7 14499.  
8  
9  
10 44. Parnas, A.; Nadler, M.; Nisemblat, S.; Horovitz, A.; Mandel, H.; Azem, A. The MitCHAP-  
11  
12 60 disease is due to entropic destabilization of the human mitochondrial Hsp60 oligomer. *J.*  
13  
14 *Biol. Chem.* **2009**, 284, 28198-28203.  
15  
16  
17 45. Fleeman, R.; LaVoi, T. M.; Santos, R. G.; Morales, A.; Nefzi, A.; Welmaker, G. S.;  
18  
19 Medina-Franco, J. L.; Giulianotti, M. A.; Houghten, R. A.; Shaw, L. N. Combinatorial  
20  
21 libraries as a tool for the discovery of novel, broad-spectrum antibacterial agents targeting  
22  
23 the ESKAPE pathogens. *J. Med. Chem.* **2015**, 58, 3340-3355.  
24  
25  
26 46. Kwasny, S. M.; Opperman, T. J. Static biofilm cultures of Gram-positive pathogens grown  
27  
28 in a microtiter format used for anti-biofilm drug discovery. *Curr. Protoc. Pharmacol.* **2010**,  
29  
30 Chapter 13, Unit 13A 18.  
31  
32  
33  
34  
35  
36  
37  
38  
39  
40  
41  
42  
43  
44  
45  
46  
47  
48  
49  
50  
51  
52  
53  
54  
55  
56  
57  
58  
59  
60

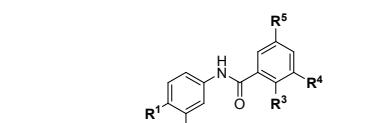
**SCHEMES, TABLES, & FIGURES****Scheme 1<sup>a</sup>**

<sup>a</sup> Reagents and conditions: a)  $\text{X} = \text{Cl}$ : pyridine,  $\text{CH}_2\text{Cl}_2$ ; b)  $\text{X} = \text{OH}$ :  $\text{SOCl}_2$ ,  $60^\circ\text{C}$ , 1 h, then concentrate and add arylamine, pyridine, and  $\text{CH}_2\text{Cl}_2$ ; c)  $\text{X} = \text{OH}$ : DCC, DMAP,  $\text{CH}_2\text{Cl}_2$ , 1 h, then add arylamine and pyridine; d)  $\text{X} = \text{OH}$ : EDC,  $\text{HOBT}\cdot\text{H}_2\text{O}$ , TEA,  $\text{CH}_2\text{Cl}_2$ ; e)  $\text{BBr}_3$ , DCM; f)  $\text{K}_2\text{CO}_3$ , EtOH; g)  $\text{K}_2\text{CO}_3$ , DMF, R.T.- $80^\circ\text{C}$ ; h) Tin powder, 10% HCl/AcOH.

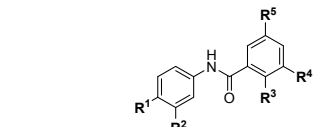
**Table 1.** Compilation of IC<sub>50</sub> results for compounds tested in the GroEL/ES-mediated dMDH and dRho refolding assays, and the native MDH and Rho reporter counter-screens.

					Biochemical Assay IC <sub>50</sub> (μM)			
					Compound # / Name	Native Rho Reporter	Native MDH Reporter	GroEL/ES-dRho Refolding
Closantel					>100	6.1	1.5	2.2
Rafoxanide					>100	25	2.2	4.3
<b>1</b>					>100	6.8	1.5	1.7
<b>2</b>					>100	>63	3.8	9.5
<b>3</b>					>100	>63	11	37
<b>4</b>					>100	>63	63	42
<b>5</b>					>100	8.4	1.3	2.7
<b>6</b>					>100	>63	14	33
<b>7</b>					>100	>63	30	38
<b>8</b>					>100	>63	87	40
<b>9</b>					>100	27	47	24
<b>10</b>					>100	>63	>100	>100
<b>11</b>					>100	>63	>100	>100
<b>12</b>					>100	>63	>100	>100
<b>13</b>					>100	51	>100	61
<b>14</b>					>100	>63	>100	>100
<b>15</b>					>100	>63	>100	>100
<b>16</b>					>100	>63	>100	>100
<b>17</b>					>100	>63	>100	>100
<b>18</b>					>100	>63	>100	>100
<b>19</b>					>100	>63	>100	>100
<b>20</b>					>100	>63	>100	>100
<b>21</b>					>100	>63	>100	>100
<b>22</b>					>100	>63	>100	>100
<b>23</b>					>100	>63	>100	>100
<b>24</b>					>100	>63	>100	>100
<b>25</b>					>100	>63	>100	>100
<b>26</b>					>100	>63	>100	>100
<b>27</b>					>100	>63	>100	>100
<b>28</b>					>100	>63	>100	>100
<b>29</b>					>100	>63	>100	>100
<b>30</b>					>100	>63	>100	>100
<b>31</b>					>100	>63	>100	>100
<b>32</b>					>100	>63	>100	>100
<b>33</b>					>100	>63	>100	>100
<b>34</b>					>100	>63	>100	>100
<b>35</b>					>100	>63	>100	>100
<b>36</b>					>100	>63	>100	>100
<b>37</b>					>100	>63	>100	>100
<b>38</b>					>100	>63	>100	>100
<b>39</b>					>100	>63	>100	>100
<b>40</b>					>100	>63	>100	>100
<b>41</b>					>100	>63	>100	>100
<b>42</b>					>100	>63	>100	>100
<b>43</b>					>100	>63	>100	>100
<b>44</b>					>100	>63	>100	>100
Vancomycin					>100	>63	>100	>100
Daptomycin					>100	>63	>100	>100
Ampicillin					>100	>63	>100	>100
Rifampicin					>100	>63	>100	>100

**Table 2.** Compilation of EC<sub>50</sub> results for compounds tested in the various bacterial proliferation assays.

		Bacterial Proliferation EC <sub>50</sub> (μM)							
		Compound # / Name	<i>E. faecium</i>	<i>S. aureus</i>		<i>K. pneumoniae</i>	<i>A. baumannii</i>	<i>P. aeruginosa</i>	<i>E. cloacae</i>
Compound Substituents & Substructures				Sensitive	Resistant				
Closantel			1.2	0.47	0.47	>100	>100	>100	>100
Rafoxanide			0.99	0.32	0.34	>100	31	>100	40
1		Cl	OH	Br	Br	>100	66	>100	>100
2		Cl	OH	Br	H	>100	2.9	>100	>100
3		Cl	OH	H	Br	>100	>100	>100	>100
4		Cl	OH	H	H	>100	>100	>100	>100
5		H	OH	Br	Br	>100	>100	>100	>100
6		H	OH	Br	H	>100	12	>100	>100
7		H	OH	H	Br	>100	>100	>100	>100
8		H	OH	H	H	>100	>100	>100	>100
9		H	Cl	OH	Br	95	46	>100	78
10		H	Cl	OH	Br	>100	>100	>100	>100
11		H	Cl	OH	H	>100	>100	>100	>100
12		H	Cl	OH	H	>100	3.1	4.2	>100
13		H	H	OH	Br	>100	1.2	2.0	>100
14		H	H	OH	Br	>100	6.4	10	>100
15		H	H	OH	H	>100	2.8	4.1	78
16		H	H	OH	H	>100	28	51	>100
17		Cl	H	Br	Br	>100	>100	>100	>100
18		Cl	H	Br (H)	H (Br)	>100	>100	>100	>100
19		Cl	H	H	H	>100	43	>100	>100
20		H	H	Br	Br	>100	>100	>100	>100
21		H	H	Br (H)	H (Br)	>100	>100	>100	>100
22		H	H	H	H	>100	>100	>100	>100
23		H	Cl	H	Br	>100	14	12	>100
24		H	Cl	H	Br (H)	>100	47	68	>100
25		H	Cl	H	H	>100	>100	>100	>100
26		H	H	H	Br	>100	>100	>100	>100
27		H	H	H	Br (H)	>100	>100	>100	>100
28		H	H	H	H	>100	>100	>100	>100
29		Cl	OCH <sub>3</sub>	Br	Br	>100	>100	>100	>100
30		Cl	OCH <sub>3</sub>	Br	H	>100	>100	>100	>100
31		Cl	OCH <sub>3</sub>	H	Br	>100	>100	>100	>100
32		Cl	OCH <sub>3</sub>	H	H	>100	>100	>100	>100
33		H	OCH <sub>3</sub>	Br	Br	>100	>100	>100	>100
34		H	OCH <sub>3</sub>	Br	H	>100	>100	>100	>100
35		H	OCH <sub>3</sub>	H	Br	>100	>100	>100	>100
36		H	OCH <sub>3</sub>	H	H	>100	>100	>100	>100
37		H	Cl	OCH <sub>3</sub>	Br	>100	46	>100	>100
38		H	Cl	OCH <sub>3</sub>	Br	>100	>100	>100	>100
39		H	Cl	OCH <sub>3</sub>	H	>100	>100	>100	>100
40		H	Cl	OCH <sub>3</sub>	H	>100	>100	>100	>100
41		H	H	OCH <sub>3</sub>	Br	>100	>100	>100	>100
42		H	H	OCH <sub>3</sub>	Br	>100	>100	>100	>100
43		H	H	OCH <sub>3</sub>	H	>100	>100	>100	>100
44		H	H	OCH <sub>3</sub>	H	>100	>100	>100	>100
Vancomycin			0.60	0.67	0.52	>100	>100	>100	>100
Daptomycin			9.2	0.68	1.0	>100	>100	>100	>100
Ampicillin			6.9	0.19	>100	>100	>100	>100	>100
Rifampicin			0.13	<0.05	0.23	11	1.3	7.8	8.8

**Table 3.** Compilation of IC<sub>50</sub> and CC<sub>50</sub> results for compounds tested in the human HSP60/10-dMDH refolding assay and the liver (THLE-3) and kidney (HEK 293) cell viability assays.

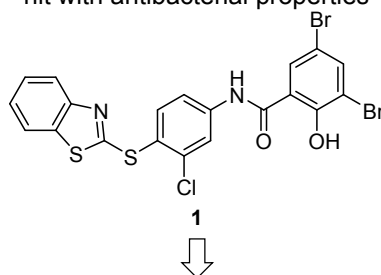
					Compound # / Name	HSP60/10-dMDH Refolding IC <sub>50</sub> (μM)	Human Cell Viability CC <sub>50</sub> (μM)	
R <sup>1</sup>	R <sup>2</sup>	R <sup>3</sup>	R <sup>4</sup>	R <sup>5</sup>			Liver (THLE-3)	Kidney (HEK 293)
Closantel						2.5	52	75
Rafoxanide						2.8	24	>100
↑								
	Cl	OH	Br	Br	<b>1</b>	4.2	14	76
	Cl	OH	Br	H	<b>2</b>	6.9	19	64
	Cl	OH	H	Br	<b>3</b>	>100	14	45
	Cl	OH	H	H	<b>4</b>	>100	34	64
↓								
	H	OH	Br	Br	<b>5</b>	4.7	20	66
	H	OH	Br	H	<b>6</b>	26	36	71
	H	OH	H	Br	<b>7</b>	>100	12	42
	H	OH	H	H	<b>8</b>	>100	33	74
↑								
	H	Cl	OH	Br	<b>9</b>	29	9.2	18
	H	Cl	OH	Br	<b>10</b>	>100	16	32
	H	Cl	OH	H	<b>11</b>	>100	4.1	15
	H	Cl	OH	H	<b>12</b>	>100	16	37
↓								
	H	H	OH	Br	<b>13</b>	63	25	34
	H	H	OH	Br	<b>14</b>	>100	56	82
	H	H	OH	H	<b>15</b>	>100	16	35
	H	H	OH	H	<b>16</b>	>100	68	>100
↑								
	Cl	H	Br	Br	<b>17</b>	>100	>100	>100
	Cl	H	Br (H)	H (Br)	<b>18</b>	>100	88	>100
	Cl	H	H	H	<b>19</b>	>100	82	90
↓								
	H	H	Br	Br	<b>20</b>	>100	>100	>100
	H	H	Br (H)	H (Br)	<b>21</b>	>100	82	74
	H	H	H	H	<b>22</b>	>100	>100	>100
↑								
	H	Cl	H	Br	<b>23</b>	>100	45	53
	H	Cl	H	Br (H)	<b>24</b>	>100	50	51
	H	Cl	H	H	<b>25</b>	>100	>100	>100
↓								
	H	H	H	Br	<b>26</b>	>100	>100	>100
	H	H	H	Br (H)	<b>27</b>	>100	>100	>100
	H	H	H	H	<b>28</b>	>100	>100	>100
↑								
	Cl	OCH <sub>3</sub>	Br	Br	<b>29</b>	>100	>100	>100
	Cl	OCH <sub>3</sub>	Br	H	<b>30</b>	>100	>100	>100
	Cl	OCH <sub>3</sub>	H	Br	<b>31</b>	>100	>100	>100
	Cl	OCH <sub>3</sub>	H	H	<b>32</b>	>100	>100	>100
↓								
	H	OCH <sub>3</sub>	Br	Br	<b>33</b>	>100	>100	>100
	H	OCH <sub>3</sub>	Br	H	<b>34</b>	>100	>100	>100
	H	OCH <sub>3</sub>	H	Br	<b>35</b>	>100	>100	>100
	H	OCH <sub>3</sub>	H	H	<b>36</b>	>100	>100	>100
↑								
	H	Cl	OCH <sub>3</sub>	Br	<b>37</b>	>100	>100	>100
	H	Cl	OCH <sub>3</sub>	Br	<b>38</b>	>100	>100	>100
	H	Cl	OCH <sub>3</sub>	H	<b>39</b>	>100	94	>100
	H	Cl	OCH <sub>3</sub>	H	<b>40</b>	>100	>100	>100
↓								
	H	H	OCH <sub>3</sub>	Br	<b>41</b>	>100	>100	>100
	H	H	OCH <sub>3</sub>	Br	<b>42</b>	>100	>100	>100
	H	H	OCH <sub>3</sub>	H	<b>43</b>	>100	>100	>100
	H	H	OCH <sub>3</sub>	H	<b>44</b>	>100	>100	>100
Vancomycin						>100	>100	>100
Daptomycin						>100	>100	>100
Ampicillin						>100	>100	>100
Rifampicin						>100	72	>100

**Table 4.** Compilation of EC<sub>50</sub> values for inhibitors tested in the biofilm formation and penetration/bactericidal activity assays.

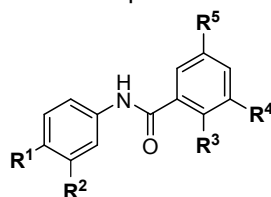
					<i>S. aureus</i> Proliferation & Biofilm Assay EC <sub>50</sub> (μM)			
Compound Substituents & Substructures					Compound # / Name	Planktonic Growth	Preventing Biofilm Formation	Killing Bacteria in Biofilms
R <sup>1</sup>	R <sup>2</sup>	R <sup>3</sup>	R <sup>4</sup>	R <sup>5</sup>				
	Cl	OH	Br	Br	<b>1</b>	0.36	0.72	2.4
	Cl	OH	Br	H	<b>2</b>	0.45	1.0	5.6
	H	OH	Br	Br	<b>5</b>	0.44	0.54	2.3
	H	OH	H	H	<b>8</b>	0.20	0.91	2.0
	H	Cl	OH	H	Br	<b>11</b>	0.46	0.44
<b>Vancomycin</b>						0.67	0.54	>100

1  
2  
3 **Figure 1. A.** Chemical structure of the initial GroEL/ES hit inhibitor, **1**, which was previously  
4 reported to potently inhibit the proliferation of *E. faecium* ( $EC_{50} = 0.15 \mu\text{M}$ ) and *S. aureus* ( $EC_{50}$   
5 =  $0.20 \mu\text{M}$ ).<sup>31</sup> Analogs of inhibitor **1** have been synthesized and evaluated in this study, where  
6 the **R**<sup>1</sup> through **R**<sup>5</sup> substituents and substructures have been systematically removed to probe for  
7 the contributions that each make to inhibiting chaperonin system biochemical functions and  
8 bacterial and human cell viabilities. **B.** Chemical structures of related compounds used as  
9 anthelmintics in veterinary medicine.

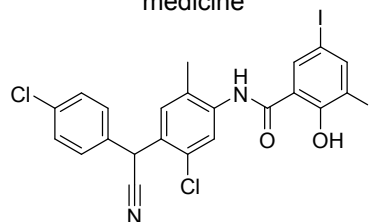
19  
20 **A.** Initial screening GroEL/ES inhibitor  
21 hit with antibacterial properties



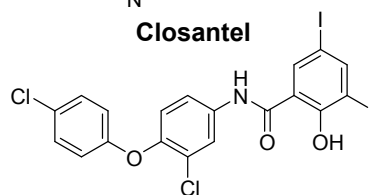
30  
31 Present study with variation at  
32 **R**<sup>1</sup>-**R**<sup>5</sup> positions



40  
41 **B.** Anthelmintics used in veterinary  
42 medicine

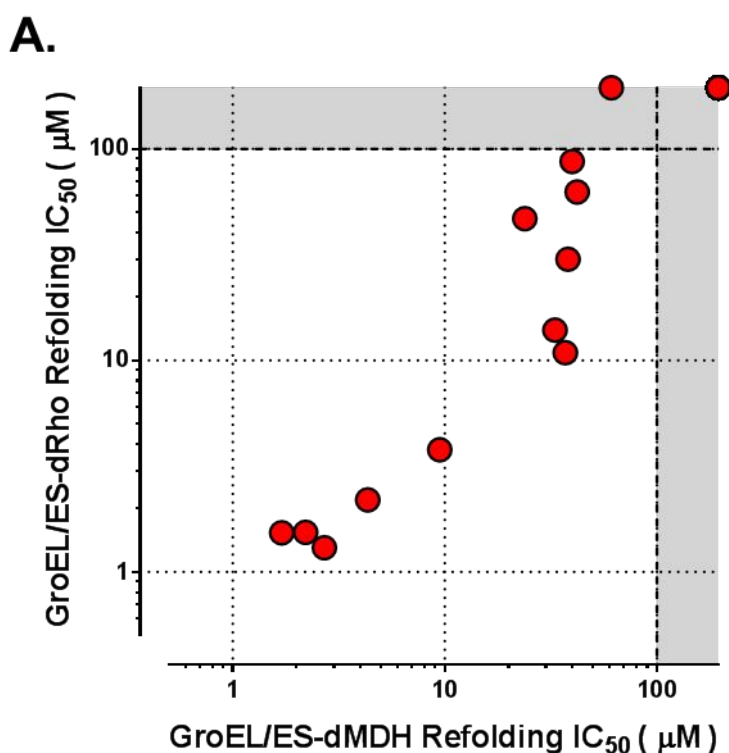


49 **Closantel**

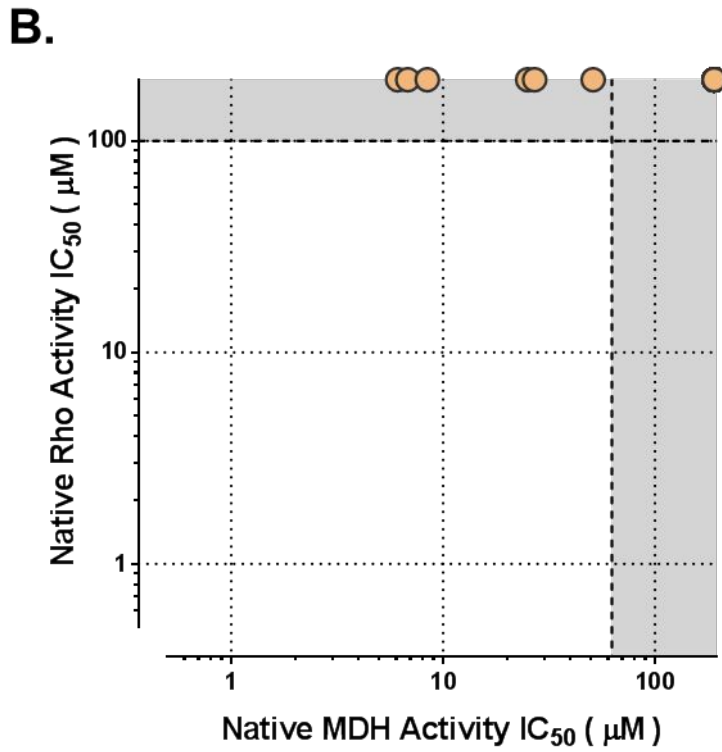


55 **Rafoxanide**

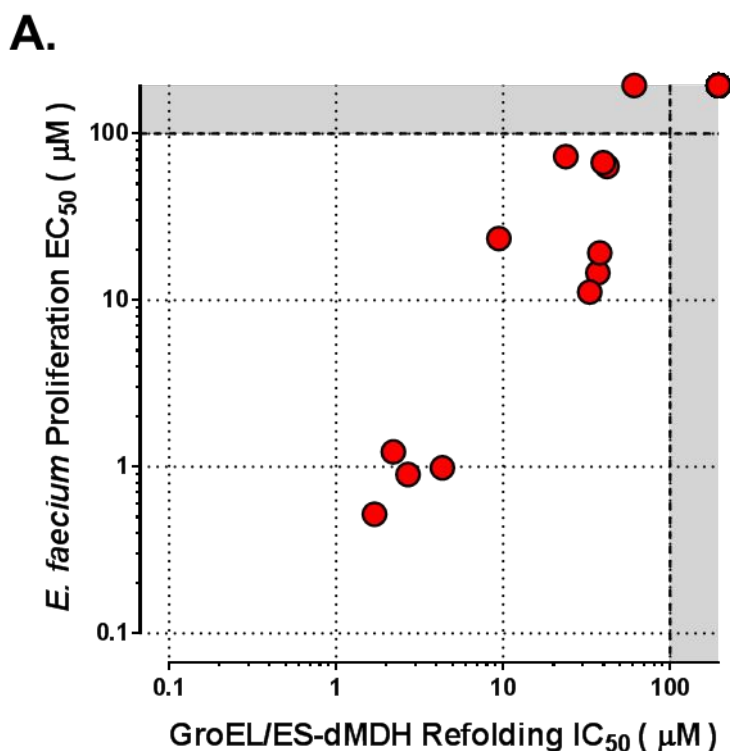
**Figure 2.** Correlation plots of  $IC_{50}$  values for compounds evaluated in the respective biochemical assays. **A.** Compounds inhibit nearly equipotently in the GroEL/ES-dMDH and the GroEL/ES-dRho refolding assays, supporting on-target effects (Spearman correlation coefficient comparing  $\log(IC_{50})$  values in each assay is 0.9663,  $p < 0.0001$ ). **B.** While some compounds inhibit in the native MDH enzymatic reporter counter screen, none inhibit native Rho enzymatic activity, further supporting on-target effects for inhibiting the chaperonin-mediated refolding cycle. Results plotted in the grey zones represent  $IC_{50}$  values higher than the maximum concentrations listed.

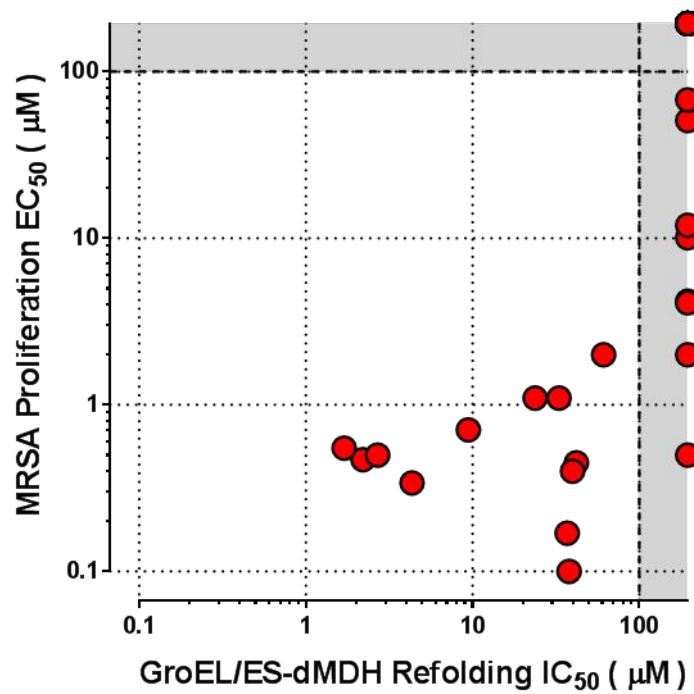




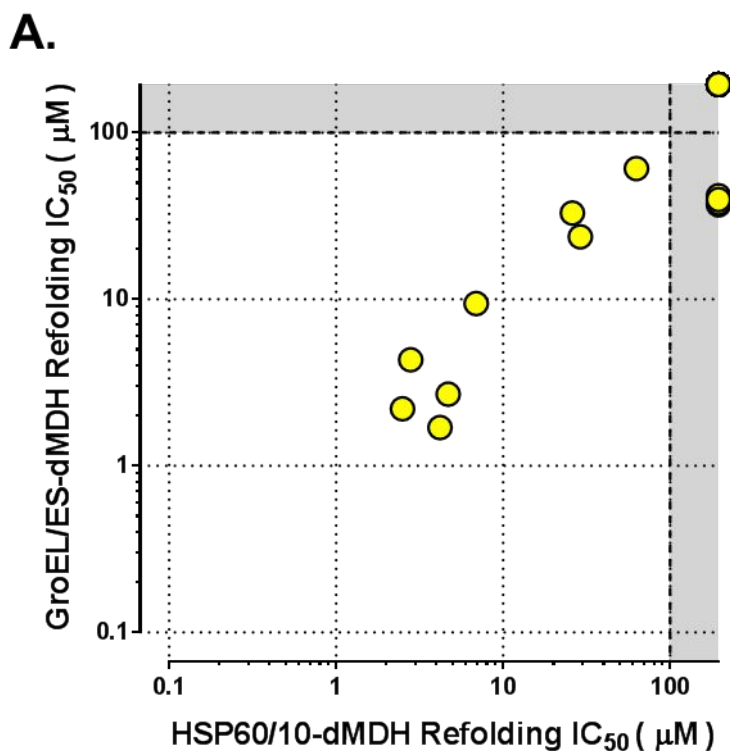


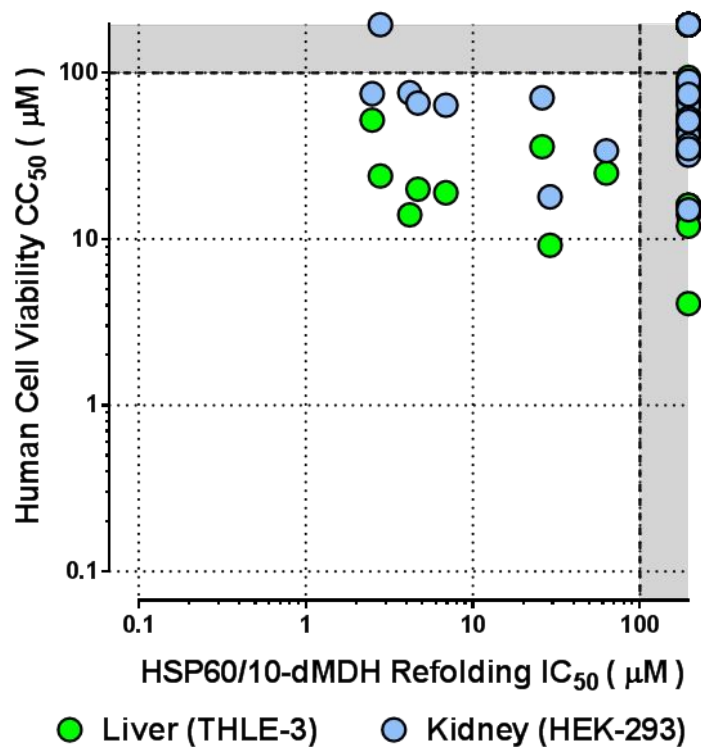
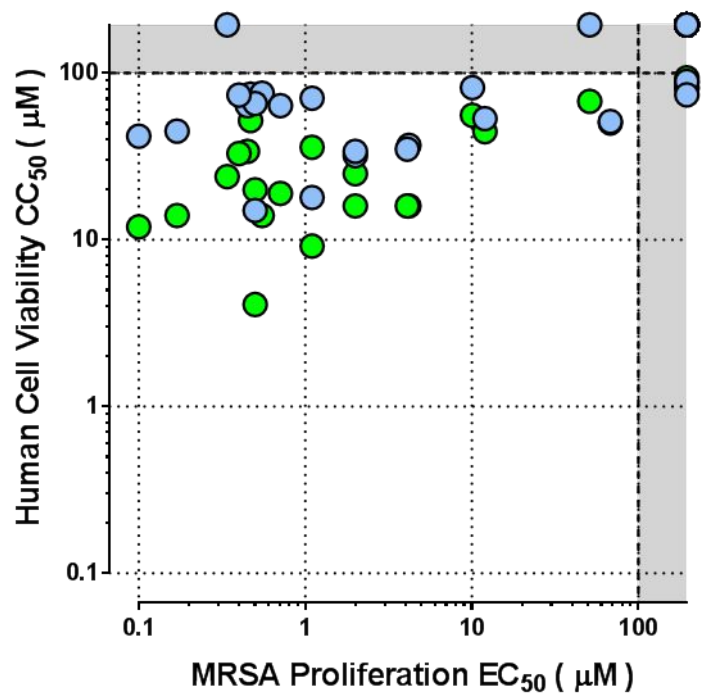
**Figure 3.** Correlation plots comparing IC<sub>50</sub> values for compounds tested in the GroEL/ES-dMDH refolding assay with EC<sub>50</sub> values for inhibiting *E. faecium* (A) and MRSA (B) proliferation. While a general trend is observed between inhibiting the GroEL/ES chaperonin system and *E. faecium* proliferation (Spearman correlation coefficient comparing log(I/EC<sub>50</sub>) values in each assay is 0.9628,  $p < 0.0001$ ), supporting on-target effects in bacteria, inhibitors are more potent against MRSA (Spearman correlation coefficient comparing log(I/EC<sub>50</sub>) values in each assay is 0.8042,  $p < 0.0001$ ), suggesting potential off-target effects and/or greater GroEL/ES sensitivity in *S. aureus* bacteria. Results plotted in the grey zones represent IC<sub>50</sub> and EC<sub>50</sub> values higher than the maximum concentrations listed.



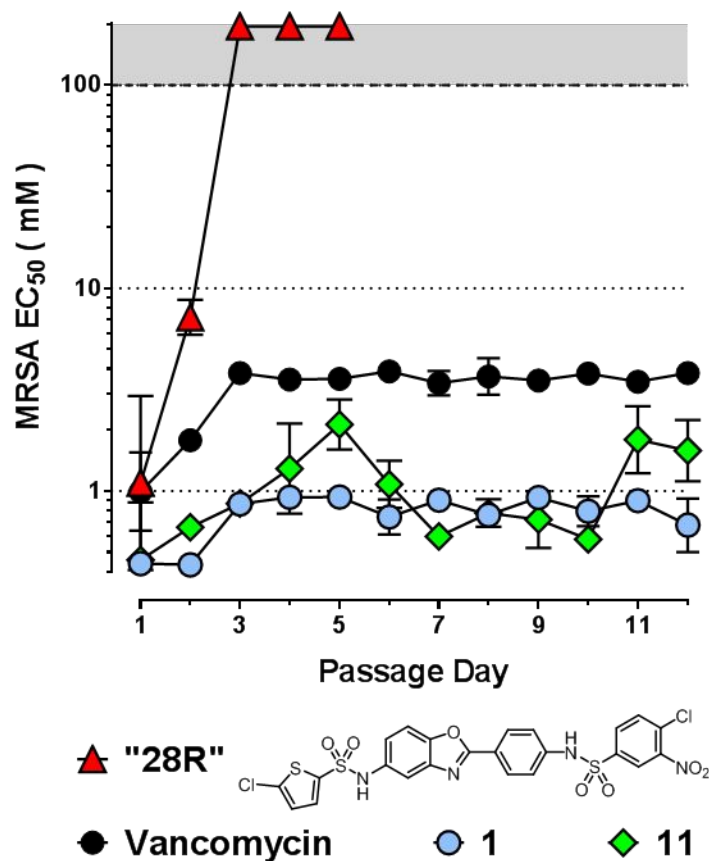
**B.**

**Figure 4.** Correlation plots comparing human HSP60/10-dMDH and GroEL/ES-dMDH refolding assay  $IC_{50}$ , human cell viability  $CC_{50}$ , and MRSA proliferation  $EC_{50}$  results. **A.** Compounds inhibit the HSP60/10 and GroEL/ES chaperonin systems nearly equipotently, suggesting binding sites may be highly conserved between the two (Spearman correlation coefficient comparing  $\log(IC_{50})$  values in each assay is 0.8351,  $p < 0.0001$ ). **B.** Despite compounds inhibiting human HSP60/10 *in vitro*, many exhibit low to no cytotoxic effects against human liver (THLE-3) and kidney (HEK 293) in cell viability assays (Spearman correlation coefficient values are 0.4791 ( $p < 0.0008$ ) and 0.3286 ( $p < 0.0258$ ) when comparing HSP60/10-dMDH refolding assay  $\log(IC_{50})$  values with liver and kidney cell viability  $\log(CC_{50})$  values, respectively). **C.** Lead analogs inhibit MRSA proliferation with high selectivity compared to cytotoxicity to human liver (THLE-3) and kidney (HEK 293) cells. Results plotted in the grey zones represent  $IC_{50}$ ,  $CC_{50}$ , and  $EC_{50}$  values higher than the maximum concentrations listed.

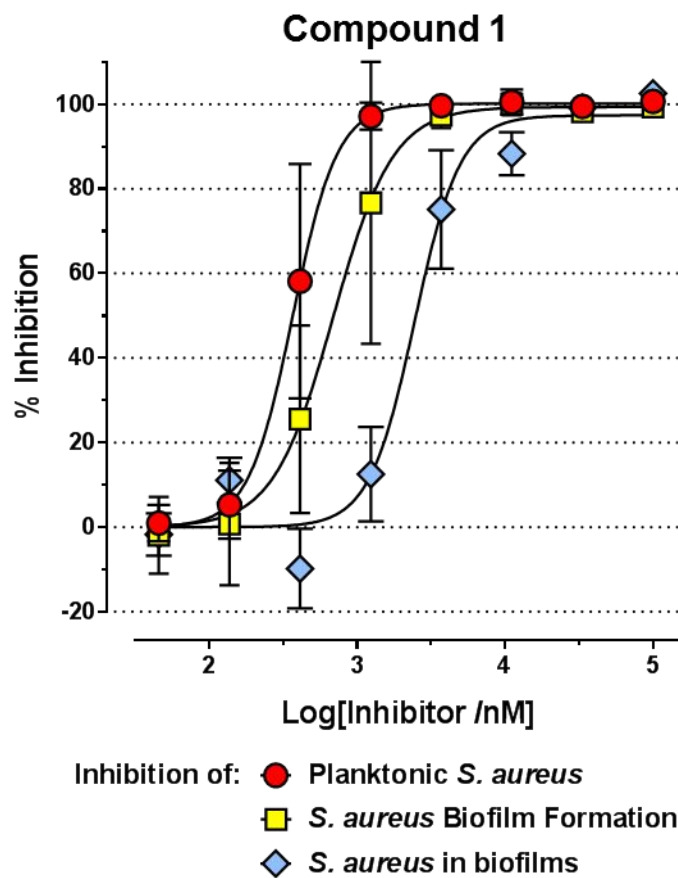


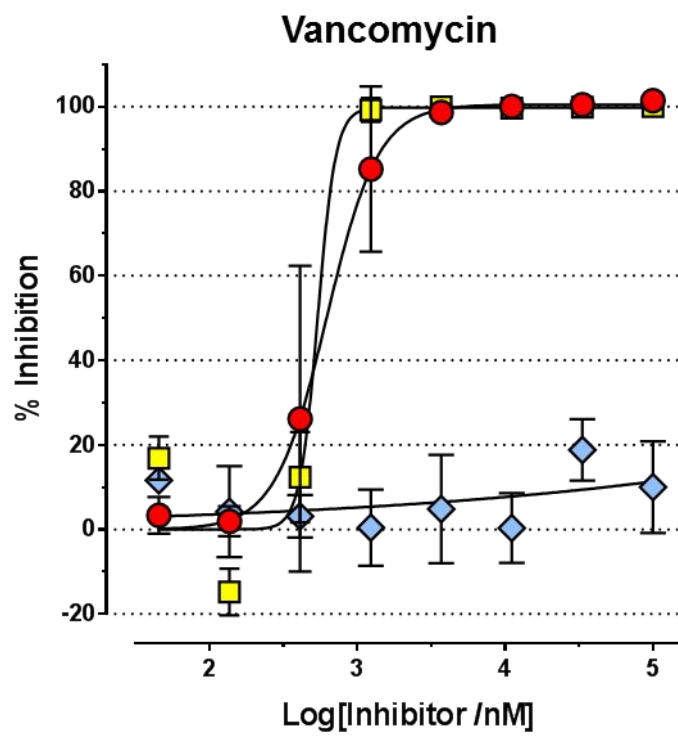
**B.****C.**

**Figure 5.** Exploring adaptive tolerance by MRSA bacteria to analogs **1**, **11**, vancomycin, and a previously-reported GroEL/ES inhibitor, “**28R**” (structure shown and numbering as previously reported).<sup>38</sup> Average  $EC_{50}$  values of compounds tested after each 24 h passage are plotted from triplicate analyses. MRSA rapidly evolved resistance to **28R**, but retained sensitivity to **1**, **11**, and vancomycin throughout 12 day experiment. Data plotted in the gray zones represent  $EC_{50}$  results beyond the assay detection limits (i.e., >100  $\mu$ M).

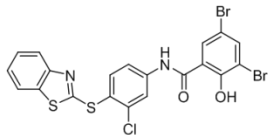
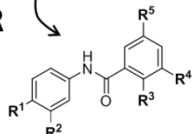
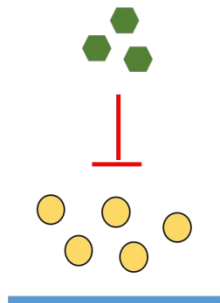
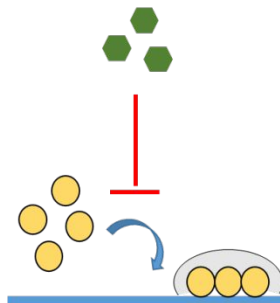


**Figure 6.** Representative dose-response plots for compound **1** (upper panel) and vancomycin (lower panel) evaluated in the *S. aureus* planktonic growth, biofilm formation, and biofilm penetration/bactericidal activity assays. Compound **1** is effective in all three assays, while vancomycin is ineffective at killing *S. aureus* bacteria in established biofilms. EC<sub>50</sub> results for **1**, vancomycin, and additional lead inhibitors tested in these assay are presented in **Table 4**.







**TABLE OF CONTENTS GRAPHIC**Initial GroEL/ES inhibitor **1****SAR**Present study varying  $R^1$ - $R^5$ Inhibits *S. aureus*  
planktonic growthInhibits *S. aureus*  
biofilm formationPenetrates and kills  
*S. aureus* within biofilm